samples were then transferred to a resin (Quetol 812; Nisshin EM Co., Tokyo, Japan) and polymerized at 60°C for 48 h. The obtained blocks were ultrathin sectioned at 70 nm with a diamond knife using an ultramicrotome (ULTRACUT UCT; Leica, Tokyo, Japan), and the sections were placed on copper grids. They were stained with 2% uranyl acetate at room temperature for 15 min and then rinsed with distilled water followed by being secondary stained with lead stain solution (Sigma-Aldrich Co.) at room temperature for 3 min.

The grids were observed by transmission electron microscopy (JEM-1200EX; JEOL Ltd., Tokyo, Japan) at an acceleration voltage of 80 kV. Digital images (2,048×2,048 pixels) were taken with a CCD camera (VELETA; Olympus Soft Imaging Solutions GmbH, Münster, Germany).

RESULTS

Cell Labeling With Magnetic Iron Oxide Nanoparticles

We developed novel magnetic iron oxide nanoparticles, electrically charged by the presence of a cationic end-group substitution of dextran (TMADM-03) (Fig. 1). In order to label cells with TMADM-03, the HepG2 cells and spheroids (2×10^5 cells) were seeded into each culture plate and incubated for 72 h at 37°C in a humidified

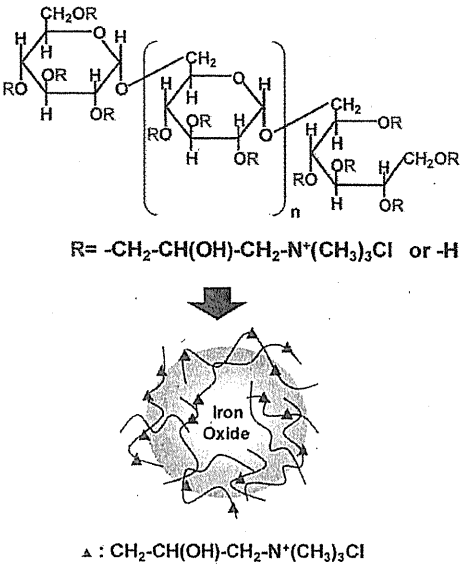

Figure 1. A schematic illustration of the magnetic iron oxide nanoparticles used in this study. The trimethylamino dextran-coated magnetic iron oxide nanoparticles (TMADM-03).

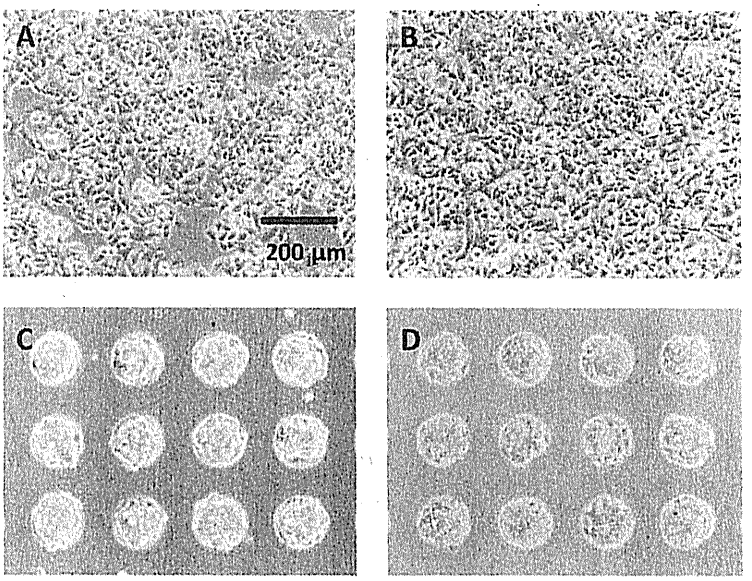

Figure 2. Phase-contrast photomicrographs of HepG2 cells and spheroids. The human hepatocellular carcinoma (HepG2) cells cultured on a standard 12-well plate (A, B) and HepG2 spheroids formed on a Cell-able 12-well plate (C, D) 72 h after inoculation. After 48 h of cell culture, the HepG2 cells were incubated with 75 μg Fe/ml TMADM-03 in culture medium for 24 h. The HepG2 cells labeled with TMADM-03 (B) and HepG2 spheroids labeled with TMADM-03 (D) are shown. Scale bar: 200 μm.

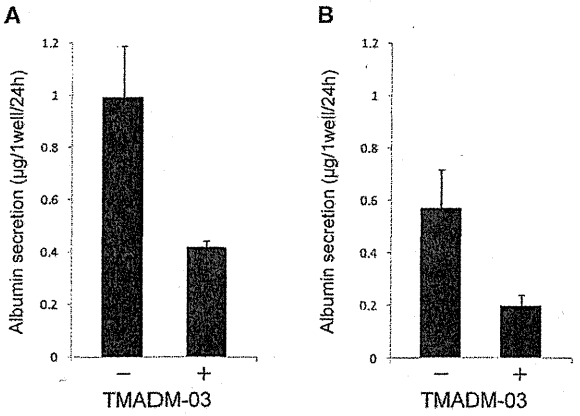

Figure 3. Albumin secretion from HepG2 cells and multicellular spheroids. (A) The HepG2 cells were incubated with 75 μg Fe/ml TMADM-03 (+) for 24 h. (B) The HepG2 spheroids were incubated with 75 μg Fe/ml TMADM-03 (+) for 24 h. As control experiments, HepG2 cells or spheroids were incubated without TMADM-03 (–) for 24 h. The data shown represent the means and SD of three independent experiments.

5% CO_2 atmosphere (Fig. 2). After incubation for 48 h, the HepG2 cells and spheroids were incubated for 24 h at 37°C in a humidified 5% CO_2 atmosphere with TMADM-03 (75 μg Fe/ml) reconstituted in culture medium (Fig. 2B and D). The morphology of both HepG2 cells and spheroids was similar to that of untransduced cells (Fig. 2A–D). However, the color of HepG2 spheroids labeled with TMADM-03 was a little darker compared with the control. The colors of HepG2 spheroids before and after labeling with TMADM-03 are shown in Figure 2C and D.

We also measured the cell viability by trypan blue exclusion assay under the conditions used for the experiments shown in Figure 2. There were very few dead cells after 72 h of cell culture (for Fig. 2A and C, the cell viability was about 95.3% and 93.6%, respectively). After the addition of TMADM-03 to the cells and incubation for 24 h, the viability was reduced compared to a 24-h incubation without TMADM-03 (for Fig. 2B and D, the cell viability was about 93.1% and 89.6%, respectively).

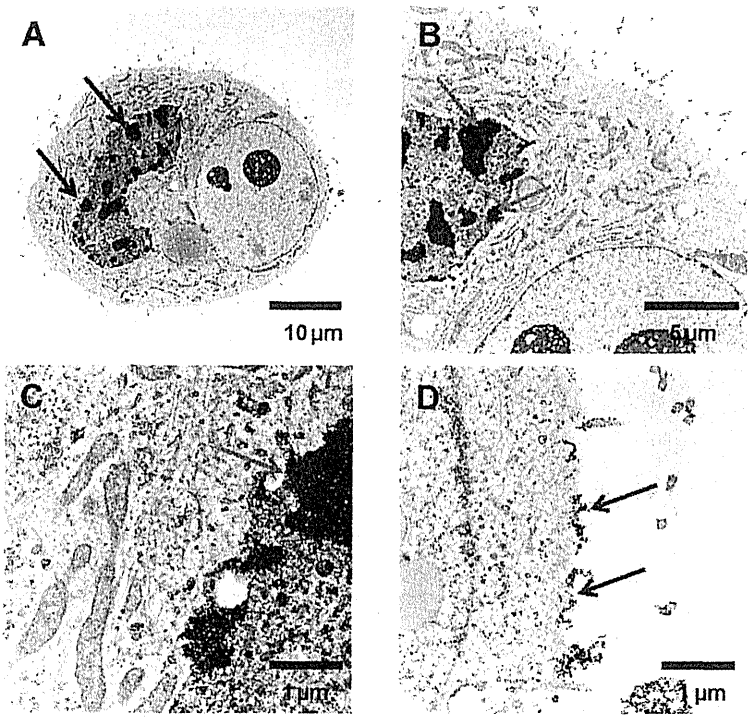

Figure 4. Transmission electron microscope (TEM) images of horizontal cross sections of HepG2 cells that had taken up TMADM-03 magnetic nanoparticles. (A) The morphology of HepG2 cells labeled with TMADM-03. The arrows point to lysosomes containing the nanoparticles (1,740×). (B) The nanoparticles (red arrow) were detected in the lysosomes (4,860×). (C) Another photograph of the nanoparticles (red arrow) in the lysosomes (18,400×) and (D) nanoparticles (blue arrows) attached to the cell membrane (18,400×).

Functional Examination of HepG2 Cells and Spheroids

To investigate the cellular function in the HepG2 spheroids, the albumin secretion was evaluated using an ELISA. The amount secreted by HepG2 cells and spheroids is shown in Figure 3A and B, respectively. The HepG2 cells and spheroids (2×10^5 cells) were incubated for 48 h at 37°C in a humidified 5% CO_2 atmosphere. After incubation for 48 h, the HepG2 cells and spheroids were incubated for another 24 h at 37°C in a humidified 5% CO_2 atmosphere with TMADM-03 (75 μg Fe/ml) reconstituted in culture medium. The albumin secretion after incubation for 24 h was reduced compared to a 24-h incubation without TMADM-03. The albumin secretion showed a decreasing trend in both the cell monolayer cultures and spheroid cultures.

TEM Images of HepG2 Cells That Had Taken Up Magnetic Nanoparticles

The incorporation of magnetic nanoparticles inside the HepG2 cells was confirmed by TEM (Fig. 4). Figure 4A shows whole images of HepG2 cells. Enlarged images of HepG2 cells are shown in Figure 4B–D. The presence of iron was confirmed after 24 h by chemical fixation, and it was found that more iron was associated with HepG2 cells in the presence of TMADM-03 than without and that this was localized in the lysosomes (Fig. 4A–C). In addition, it was located closer to the cell membrane (Fig. 4D).

TEM Images of Horizontal Cross Sections of HepG2 Spheroids That Had Taken Up Magnetic Nanoparticles

After incubation for 48 h, the HepG2 spheroids were incubated for 24 h at 37°C in a humidified 5% CO_2 atmosphere with TMADM-03 (75 μg Fe/ml) reconstituted in culture medium. Each sample was prepared in a planar direction to HepG2 spheroids on patterned cell array glass disks. The presence of iron was confirmed by TEM (Fig. 5). The incorporation of magnetic nanoparticles inside the HepG2 spheroids was confirmed (Fig. 5). Figure 5A shows a whole image of HepG2 spheroids. The enlarged images of HepG2 spheroids are shown in Figure 5B–D. In addition, magnetic iron oxide nanoparticles could be observed in the deeper layers of the spheroids (Fig. 5A), and these were localized mainly in the lysosomes (Fig. 5B–D).

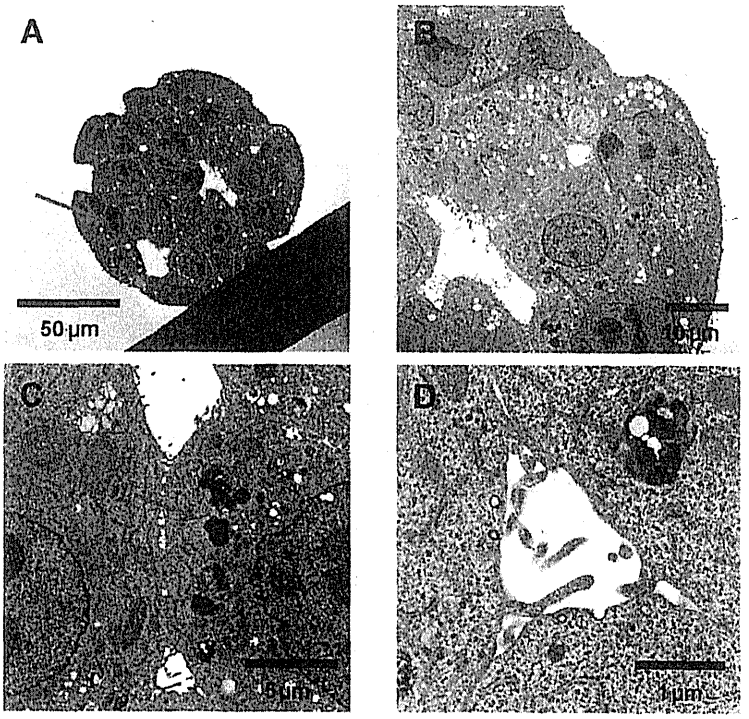

Figure 5. TEM images of horizontal cross sections of HepG2 spheroids that had taken up TMADM-03 magnetic nanoparticles. (A) Each sample was prepared in a planar direction to the patterned cell array glass disks. The morphology of HepG2 spheroids labeled with TMADM-03 is shown. The red arrows point to lysosomes containing the nanoparticles (579×). (B) A photograph showing the nanoparticles (red arrow) localized in the lysosomes (1,740×). (C) Another photograph of the nanoparticles (red arrow) in the lysosomes (4,860×). (D) A higher magnification photograph showing nanoparticles (red arrow) in the lysosomes (18,400×).

TEM Images of Vertical Cross Sections of HepG2 Spheroids That Had Taken Up Magnetic Nanoparticles

Each sample was prepared in a vertical direction to HepG2 spheroids on patterned cell array glass disks. Figure 6A shows a whole image of HepG2 spheroids. Enlarged images of HepG2 spheroids are shown in Figure 6B–D. Magnetic iron oxide nanoparticles could be observed in the deeper layers of the spheroids (Fig. 6A) by TEM. The iron was detected in the lysosomes (Fig. 6B–D).

DISCUSSION

To observe cells and tissues posttransplantation, they can be labeled with magnetic metallic oxides, such as SPIO before transplantation, and then tracked by MRI (1,2,4–6, 8,9,11,14,15,19,24,27). Techniques for visualizing therapeutic cells used for cell therapy is highly sought after since a patient's postoperative course can thus be monitored noninvasively. It has been proposed that cells can be labeled using a complex of polysaccharides, such as magnetic metallic oxides–dextran. For example, it was reported that magnetic metallic oxide nanoparticles covered with diethylamino-dextran (3) and surface-modified iron oxide nanoparticles (IONs) were obtained by coprecipitating a pullulan and its derivatives in an ammonium aqueous solution of Fe^{2+}/Fe^{3+} (12). However, commercially available magnetic nanoparticles are not efficiently transduced into cells. In previous reports, we described the novel magnetic iron oxide nanoparticles, which are electrically charged by the presence of a cationic end-group substitution of dextran (21,22).

Novel magnetic iron oxide nanoparticles improve the efficiency of their uptake into MIN6 cells (22). These nanoparticles could be used to observe transplanted cells inside the body (data not shown). In experiments using in vitro models, we observed the localization of nanoparticles in greater detail, specifically within 3D models, which mimic environments close to that of natural tissues using the Cell-able plates. Albumin secretion by HepG2 cells incubated with TMADM-03 was lower than by those incubated without TMADM-03 in 2D and 3D cultures. The decrease in albumin secretion might be due to the suppressed cell proliferation.

In the present study, TMADM-03 was efficiently incorporated into HepG2 spheroids. We observed TEM image

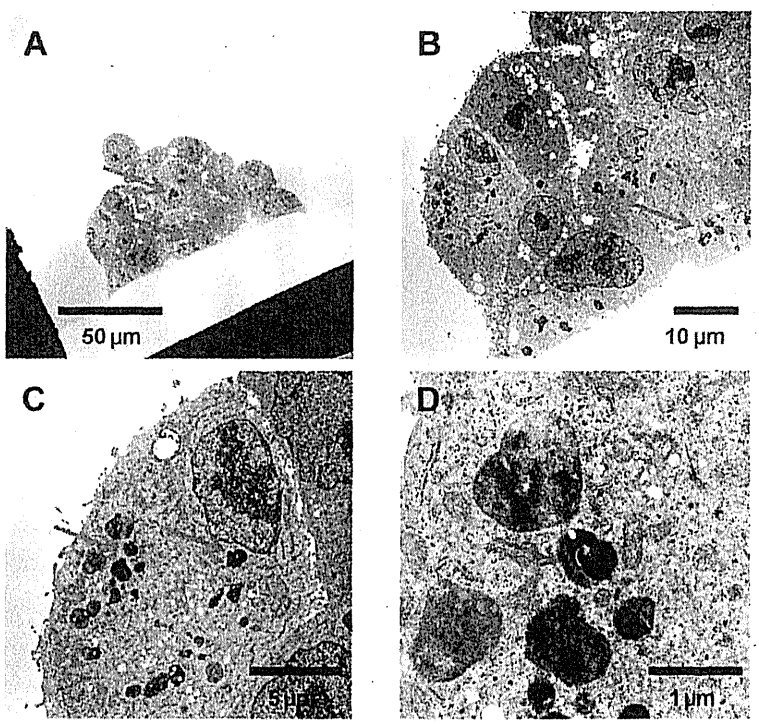

Figure 6. TEM images of vertical cross sections of HepG2 spheroids that had taken up TMADM-03 magnetic nanoparticles. (A) Each sample was prepared in a vertical direction to the patterned cell array glass disks. The morphology of HepG2 spheroids labeled with TMADM-03. The arrows point to lysosomes containing the nanoparticles (579×). (B) Another photograph of the nanoparticles (red arrow) localized in the lysosomes (1,740×). (C) An enlarged photograph showing the nanoparticles (red arrow) in the lysosomes (4,860×). (D) A high magnification photograph showing the nanoparticles (red arrow) detected in the lysosomes (18,400×).

samples that were prepared in a planar direction or a vertical direction to the HepG2 spheroids. The incorporation of TMADM-03 could be confirmed in the deeper layers of the spheroids, and the nanoparticles were observed on sections of both the planar direction and vertical direction. In addition, TMADM-03 nanoparticles were localized in the lysosomes of the HepG2 spheroids. Both HepG2 cells (2D cultures) and HepG2 spheroids (3D cultures) showed a tendency for the TMADM-03 nanoparticles to be introduced mainly into the lysosomes.

In conclusion, we observed HepG2 spheroids, which mimic an environment close to that of natural tissues, and examined, in detail, the localization of TMADM-03. Results obtained using this evaluation system are expected to be useful for drug development applications employing the Cell-able plates.

ACKNOWLEDGMENTS: We would like to thank Ms. Rina Yokota (Nagoya University) for her technical assistance and Tokai Electron Microscopy, Inc., for technical support. The present work was supported in part by Research for Promoting Technological Seeds from Japan Science and Technology Agency. The authors declare no conflict of interest.

REFERENCES

1. Barnett, B. P.; Arepally, A.; Karmarkar, P. V.; Qian, D.; Gilson, W. D.; Walczak, P.; Howland, V.; Lawler, L.; Lauzon, C.; Stuber, M.; Kraitchman, D. L.; Bulte, J. W. Magnetic resonance-guided, real-time targeted delivery and imaging of magnetocapsules immunoprotecting pancreatic islet cells. Nat. Med. 13(8):986–991; 2007.
2. Bulte, J. W.; Zhang, S.; van Gelderen, P.; Herynek, V.; Jordan, E. K.; Duncan, I. D.; Frank, J. A. Neurotransplantation of magnetically labeled oligodendrocyte progenitors: Magnetic resonance tracking of cell migration and myelination. Proc. Natl. Acad. Sci. USA 96(26):15256–15261; 1999.
3. Chouly, C.; Pouliquen, D.; Lucet, I.; Jeune, J. J.; Jallet, P. Development of superparamagnetic nanoparticles for MRI: Effect of particle size, charge and surface nature on biodistribution. J. Microencapsul. 13(3):245–255; 1996.
4. Dodd, C. H.; Hsu, H. C.; Chu, W. J.; Yang, P.; Zhang, H. G.; Mountz, J. D. Jr.; Zinn, K.; Forder, J.; Josephson, L.; Weissleder, R.; Mountz, J. M.; Mountz, J. D. Normal T-cell response and in vivo magnetic resonance imaging of T cells loaded with HIV transactivator-peptide-derived superparamagnetic nanoparticles. J. Immunol. Methods 256(1–2):89–105; 2001.
5. Dodd, S. J.; Williams, M.; Suhan, J. P.; Williams, D. S.; Koretsky, A. P.; Ho, C. Detection of single mammalian cells by high-resolution magnetic resonance imaging. Biophys. J. 76(1 Pt 1):103–109; 1999.
6. Dousset, V.; Delalande, C.; Ballarino, L.; Quesson, B.; Seilhan, D.; Coussemacq, M.; Thiaudiére, E.; Brochet, B.; Canioni, P.; Caillé, J. M. In vivo macrophage activity imaging in the central nervous system detected by magnetic resonance. Magn. Reson. Med. 41(2):329–333; 1999.
7. Enosawa, S.; Miyamoto, Y.; Hirano, A.; Suzuki, S.; Kato, N.; Yamada, Y. Application of cell array 3D-culture system for cryopreserved human hepatocytes with low-attaching capability. Drug Metab. Rev. 39(Suppl.1):342; 2007.
8. Evgenov, N. V.; Medarova, Z.; Dai, G.; Bonner-Weir, S.; Moore, A. In vivo imaging of islet transplantation. Nat. Med. 12(1):144–148; 2006.
9. Evgenov, N. V.; Medarova, Z.; Pratt, J.; Pantazopoulos, P.; Leyting, S.; Bonner-Weir, S.; Moore, A. In vivo imaging of immune rejection in transplanted pancreatic islets. Diabetes 55(9):2419–2428; 2006.
10. Huang, H.; Hanada, S.; Kojima, N.; Sakai, Y. Enhanced functional maturation of fetal porcine hepatocytes in three-dimensional poly-L-lactic acid scaffolds: A culture condition suitable for engineered liver tissues in large-scale animal studies. Cell Transplant. 15(8–9):799–809; 2006.
11. Jirák, D.; Kríz, J.; Herynek, V.; Andersson, B.; Girman, P.; Burian, M.; Saudek, F.; Hájek, M. MRI of transplanted pancreatic islets. Magn. Reson. Med. 52(6):1228–1233; 2004.
12. Jo, J.; Aoki, I.; Tabata, Y. Design of iron oxide nanoparticles with different sizes and surface charges for simple and efficient labeling of mesenchymal stem cells. J. Control. Release. 142(3):465–473; 2010.
13. Kinoshita T, Miyajima A. Cytokine regulation of liver development. Biochim. Biophys. Acta. 1592(3):303–312; 2002.
14. Kriz, J.; Jirák, D.; Girman, P.; Berková, Z.; Zacharovova, K.; Honsova, E.; Lodererova, A.; Hajek, M.; Saudek, F. Magnetic resonance imaging of pancreatic islets in tolerance and rejection. Transplantation 80(11):1596–1603; 2005.
15. Lewin, M.; Carlesso, N.; Tung, C. H.; Tang, X. W.; Cory, D.; Scadden, D. T.; Weissleder, R. Tat peptide-derivatized magnetic nanoparticles allow in vivo tracking and recovery of progenitor cells. Nat. Biotechnol. 18(4):410–414; 2000.
16. Miyamoto, Y.; Enosawa, S.; Takeuchi, T.; Takezawa, T. Cryopreservation *in situ* of cell monolayers on collagen vitrigel membrane culture substrata: Ready-to-use preparation of primary hepatocytes and ES cells. Cell Transplant. 18:619–626; 2009.
17. Miyamoto, Y.; Ikeya, T.; Enosawa, S. Preconditioned cell array optimized for a three-dimensional culture of hepatocytes. Cell Transplant. 18:677–681; 2009.
18. Miyamoto, Y.; Koshidaka, Y.; Noguchi, H.; Oishi, K.; Saito, H.; Yukawa, H.; Kaji, N.; Ikeya, T.; Iwata, H.; Baba, Y.; Murase, K.; Hayashi, S. Polysaccharide functionalized magnetic nanoparticles for cell labeling and tracking: A new three-dimensional cell-array system for toxicity testing. In: Nagarajan, R., ed. Nanomaterials for Biomedicine. Washington, DC: ACS Publications;2012:191–208.
19. Moore, A.; Sun, P. Z.; Cory, D.; Högemann, D.; Weissleder, R.; Lipes, M. A. MRI of insulitis in autoimmune diabetes. Magn. Reson. Med. 47(4):751–758; 2002.
20. Noguchi, H.; Iwanaga, Y.; Okitsu, T.; Nagata, H.; Yonekawa, Y.; Matsumoto, S. Evaluation of islet transplantation from non-heart beating donors. Am. J. Transplant. 6(10):2476–2482; 2006.
21. Oishi, K.; Noguchi, H.; Saito, H.; Yukawa, H.; Miyamoto, Y.; Murase, K.; Hayashi, S. Cell labeling with a novel contrast agent of magnetic resonance imaging. Cell Transplant. 19(6):887–892; 2010.
22. Oishi, K.; Noguchi, H.; Saito, H.; Yukawa, H.; Miyamoto, Y.; Ono, K.; Murase, K.; Sawada, M.; Hayashi, S. Novel positive-charged nanoparticles for efficient magnetic resonance imaging of islet transplantation. Cell Med. 3(1–3):43–49; 2012.
23. Otsuka, H.; Hirano, A.; Nagasaki, Y.; Okano, T.; Horiike, Y.; Kataoka, K. Two-dimensional multiarray formation of hepatocytes spheroids on a microfabricated PEG-brush surface. Chembiochem 5:850–855; 2004.

24. Saudek, F.; Jirák, D.; Girman, P.; Herynek, V.; Dezortová, M.; Kríz, J.; Peregrin, J.; Berková, Z.; Zacharovová, K.; Hájek, M. Magnetic resonance imaging of pancreatic islets transplanted into the liver in humans. Transplantation 90(12):1602–1606; 2010.
25. Shapiro, A. M.; Lakey, J. R.; Ryan, E. A.; Korbutt, G. S.; Toth, E.; Warnock, G. L.; Kneteman, N. M.; Rajotte, R. V. Islet transplantation in seven patients with type 1 diabetes mellitus using a glucocorticoid-free immunosuppressive regimen. N. Engl. J. Med. 343(4):230–238; 2000.
26. Shapiro, A. M.; Ricordi, C.; Hering, B. J.; Auchincloss, H.; Lindblad, R.; Robertson, R. P.; Secchi, A.; Brendel, M. D.; Berney, T.; Brennan, D. C.; Cagliero, E.; Alejandro, R.; Ryan, E. A.; DiMercurio, B.; Morel, P.; Polonsky, K. S.; Reems, J. A.; Bretzel, R. G.; Bertuzzi, F.; Froud, T.; Kandaswamy, R.; Sutherland, D. E.; Eisenbarth, G.; Segal, M.; Preiksaitis, J.; Korbutt, G. S.; Barton, F. B.; Viviano, L.; Seyfert-Margolis, V.; Bluestone, J.; Lakey, J. R. International trial of the Edmonton protocol for islet transplantation. N. Engl. J. Med. 355(13):1318–1330; 2006.
27. Tai, J. H.; Foster, P.; Rosales, A.; Feng, B.; Hasilo, C.; Martinez, V.; Ramadan, S.; Snir, J.; Melling, C. W.; Dhanvantari, S.; Rutt, B.; White, D. J. Imaging islets labeled with magnetic nanoparticles at 1.5 Tesla. Diabetes 55(11):2931–2938; 2006.

Cell Medicine, Vol. 5, pp. 53–57, 2013
Printed in the USA.

2155-1790/13 $90.00 + .00
DOI: http://dx.doi.org/10.3727/215517913X666512
www.cognizantcommunication.com

Review

ER Stress and β-Cell Pathogenesis of Type 1 and Type 2 Diabetes and Islet Transplantation

Hitomi Usui Kataoka* and Hirofumi Noguchi†

*Department of Primary Care and Medical Education, Okayama University Graduate School of Medicine, Dentistry and Pharmaceutical Sciences, Okayama, Japan
†Department of Surgery, Clinical Research Center, Chiba-East Hospital, National Hospital Organization, Chiba, Japan

Endoplasmic reticulum (ER) stress affects the pathogenesis of diabetes. ER stress plays important roles, both in type 1 and type 2 diabetes, because pancreatic β-cells possess highly developed ER for insulin secretion. This review summarizes the relationship between ER stress and the pathogenesis of type 1 and type 2 diabetes. In addition, the association between islet transplantation and ER stress is discussed.

Key words: β-Cells; Endoplasmic reticulum (ER) stress; Islet transplantation

ER STRESS IN DIABETES

Diabetes mellitus is a devastating disease, and the World Health Organization (WHO) expects that the number of diabetic patients worldwide will increase to 300 million by 2025. Type 1 diabetes results from autoimmune-mediated destruction of insulin-secreting β-cells of the pancreas, whereas type 2 diabetes is associated with systemic insulin resistance and reduced insulin secretion by β-cells. Type 1 diabetes develops when β-cells are selectively disrupted by autoimmune and/or inflammatory processes. Type 2 diabetes occurs when both functional defects and reduced β-cell mass contribute to β-cell dysfunction. Apoptosis in β-cells is detected in both type 1 diabetes and type 2 diabetes (4). Hyperlipidemia and hyperglycemia are likely causes of β-cell apoptosis (8,20,27,34). Pancreatic β-cells produce insulin in response to fluctuations in blood glucose levels. There is a constant demand from the body for insulin biosynthesis and secretion, so baseline endoplasmic reticulum (ER) stress levels are high in these cells. Evidence suggests that cellular stress caused by the accumulation of unfolded and misfolded proteins in the ER is related to β-cell dysfunction and death during the development and progression of type 1 and type 2 diabetes (9,10,32).

The ER is an organelle that has several important functions, such as posttranslational modification, folding and assembly of newly synthesized secretory proteins, and storing cellular calcium (Ca^{2+}). Pancreatic β-cells possess a highly developed ER, required for the folding, export, and processing of newly synthesized insulin. Human preproinsulin is synthesized in the cytoplasm, translocated into the lumen of the ER, and cleaved to produce proinsulin. Proinsulin undergoes protein folding in the lumen of the ER. Properly folded proinsulin is then delivered to the Golgi apparatus and packed into secretory granules (23). The conversion of proinsulin to insulin takes place in the secretory granules, and mature insulin is released by exocytosis (28). ER homeostasis must be maintained in order for secretory proteins to fold properly. Various conditions that disturb ER function result in stress that causes the accumulation of misfolded proteins in the ER (2,28,42). ER function can be impaired by viral infections, environmental toxins, inflammatory cytokines, and mutant protein expression, as well as by physiological processes

Received June 1, 2012; final acceptance May 1, 2013. Online prepub date: May 14, 2013.
Address correspondence to Hitomi Usui Kataoka, M.D., Ph.D., Department of Primary Care and Medical Education, Okayama University Graduate School of Medicine, Dentistry and Pharmaceutical Sciences, 2-5-1 Shikata-cho, Okayama 700-8558, Japan. Tel: +81-86-235-6963; Fax: +81-86-221-6963; E-mail: hitomik@md.okayama-u.ac.jp *or* Hirofumi Noguchi, M.D., Ph.D., Department of Surgery, Clinical Research Center, Chiba-East National Hospital, National Hospital Organization, 673 Nitona, Chuo-ku, Chiba 260-8712, Japan. Tel: +81-43-261-5171; Fax: +81-43-268-2613; E-mail: n.hirofumi@cehpnet.com *or* noguchih2006@yahoo.co.jp

such as aging and the large biosynthetic load placed on the ER such as due to insulin production in response to blood glucose fluctuations.

Cells have a self-protective mechanism, known as the ER stress response or unfolded protein response (UPR), that allows them to survive under ER stress conditions. That mechanism involves [1] translational attenuation, which reduces synthesis of new protein and prevents further accumulation of unfolded proteins; [2] upregulation of the genes encoding ER chaperone proteins to increase protein folding activity and to prevent protein aggregation; [3] proteosomal degradation of misfolded proteins following their regulated extrusion from the ER; and [4] apoptosis in the event of persistent stress (28,29). The UPR either protects β-cells or promotes their death, depending on the nature of the stress condition. The UPR induces apoptosis when ER function is severely impaired. Signaling from the ER is initiated by ER-localized stress sensors, protein kinase RNA (PKR)-like ER kinase (PERK), activating transcription factor (ATF)6, and inositol-requiring kinase (IRE)1, which remain inactive under nonstress conditions due to association of their ER luminal domains with binding protein (BiP) (3). Apoptosis is induced by ATF4 transcriptional activation of the gene for cytidine-cytidine-adenosine-adenosine-thymidine (CCAAT)/enhancer-binding protein (C/EBP) homologous protein (CHOP) (24,39) and by activation of c-Jun N-terminal kinase 1 (JNK1) and caspase-12 (2,28,42).

ER Stress and Type 1 Diabetes

Pancreatic β-cells are the target of an autoimmune assault in type 1 diabetes, with invasion of the islets by mononuclear cells in an inflammatory reaction termed "insulitis," leading to loss of most β-cells after prolonged periods of disease (16). Both animal models and human type 1 diabetes show that β-cell apoptosis coincides with expression of cytokines such as interleukin (IL)-1β, interferon (IFN)-γ, and tumor necrosis factor (TNF)-α by the infiltrating immune cells and inducible nitric oxide (NO) synthase (iNOS) by both β-cells and immune cells (14,36). However, the complete mechanisms causing β-cell destruction have not been clarified. Recent studies have proposed that the mechanism of cytokine-induced β-cell death involves ER stress. β-cells are characterized by highly developed ER, which is important for insulin secretion. β-Cells represent one of the tissues most susceptible to ER stress (2). The baseline of ER stress in β-cells is higher than that of other cell types due to their exposure to frequent energy fluctuations, constant demand of insulin biosynthesis, and secretion (10). Viral infections, environmental stresses, as well as NO are insults to the β-cell that can lead to excessive, unresolved ER stress, thus triggering an apoptotic cascade (23).

Oydomari et al. revealed the mechanism of β-cell damage by ER stress. They used mouse insulinoma 6 (MIN6) cells, a mouse β-cell-derived cell line. They showed that CHOP, a C/EBP homologous protein, is induced by a NO donor and leads to apoptosis. They concluded that NO depletes ER Ca^{2+}, causes ER stress, and leads to β-cell apoptosis. Ca^{2+} is required for the protein binding and chaperoning ability of ER chaperones (25). Severe ER Ca^{2+} depletion will impair the quality of ER protein folding and trigger CHOP expression and apoptosis. Cardozo et al. reported that production of NO leads to the attenuation of the sarcoendoplasmic reticulum pump Ca^{2+} ATPase2b (SERCA2b) and consequently the reduction of Ca^{2+} in the ER. This Ca^{2+} depletion leads to severe ER stress and the induction of the proapoptotic transcription factor CHOP. They suggested that IL-1β and IFN-γ-induced decrease in SERCA2b expression, with subsequent depletion of ER Ca^{2+} and activation of the ER stress pathway, is a potential contributory mechanism to β-cell death (5). In addition, Wang et al. suggested that the IL-1β-induced depletion of ER Ca^{2+} and activation of the ER stress via the JNK pathway are potential mechanisms that contribute to β-cell death (38).

On the other hand, there are studies that suggest that the PERK-ATF4-CHOP ER stress-signaling pathway is not required for cytokine-induced β-cell death (1). Although more studies and new insights are expected to clarify the mechanism of β-cell apoptosis in type 1 diabetes, it is clear that ER stress plays important roles in β-cell dysfunction.

ER Stress and Type 2 Diabetes

Resistance to insulin action in peripheral tissues, such as adipose tissue, muscle, and liver, is one of the primary presenting features of type 2 diabetes. This insulin resistance leads to the hyperproduction of insulin in the β-cell. Hyperglycemia and type 2 diabetes develop in patients who are unable to sustain this compensatory response of the β-cell. This high insulin production exceeds the ER folding capacity and leads to severe, chronic hyperactivation of the UPR, inducing β-cell apoptosis. This phenomenon is associated with chronic activation of IRE1 during consistent insulin biosynthesis, which leads to activation of the IRE1-JNK proapoptotic signaling pathway (37). ER stress has been proposed to be the cellular/molecular mechanism linking obesity with insulin resistance (6). Ozcan et al. showed that obesity can cause ER stress. It leads to the suppression of insulin receptor signaling through hyperactivation of JNK and subsequent serine phosphorylation of insulin receptor substrate-1 (IRS-1) (26). Several studies have indicated that ER stress is an early consequence of nutrient excess and a cause for the development of insulin resistance and inflammation. Chronic excess nutrient intake has been shown to cause

ER stress, as well as insulin resistance and inflammation in the adipose tissue of ob/ob mice and in mice with high-fat diets (11).

CHOP is also induced by ER stress and has a central role in its apoptotic execution pathways. A recent study revealed that systemic deletion of CHOP induced abdominal obesity and hepatic steatosis, with normal glucose tolerance and insulin sensitivity, and revealed lower levels of proinflammatory cytokines and less infiltration of immune cells into fat and liver. It indicated that insulin resistance is not induced by fat accumulation, but rather by the inflammation induced by ectopic fat, and CHOP may take important role in inflammation that induce insulin resistance (21). Free fatty acids (FFAs) might also be responsible for the ER stress response observed in the hepatocytes or adipocytes of obese mice (22,26), while simultaneously disturbing pancreatic β-cell function and viability. Furthermore, Laybutt demonstrated that the proapoptotic fatty acid palmitate triggers a comprehensive ER stress response in MIN6 cells, as well as the activation of genes involved in ER stress, in islets from db/db mice and from human type 2 diabetes subjects (18). In addition, Sage et al. suggested that ER stress was elevated in monocytes isolated from individuals with metabolic syndrome (31). Monocytes play an important role in causing insulin resistance and vascular complications. These findings suggest that there is an association between both acute and chronic hyperglycemia and ER stress in humans.

ER STRESS AND ISLET TRANSPLANTATION

Controlling the blood glucose level is therefore critical for preventing vascular complications in diabetes and maintaining the function of β-cells. However, it is difficult to achieve the optimal control. The Third National Health and Nutrition Examination Survey (NHANES III) showed that only 50% of diabetics achieve a glycated hemoglobin (HbA1c) level of less than 7%. The only way to ensure the long-term health of diabetic patients is to maintain constant normoglycemia. However, despite intensive insulin therapy, most individuals with type 1 diabetes are unable to maintain a blood glucose level in the optimal range. In addition, intensive insulin therapy is associated with an increased risk of hypoglycemia. Pancreatic islet transplantation has emerged as one of the most promising therapeutic approaches for improving glycometabolic control in type 1 diabetic patients (12). The "Edmonton Protocol" introduced several modifications to the transplantation procedure, such as the use of a steroid-free immunosuppression regimen and transplantation of a mean islet mass of 11,000 IEQ/kg of a patient's weight (33). Clinical islet transplantation activity has dramatically increased all over the world. However, the Edmonton group showed that only 7.5% of the 65 patients who received islet transplantation achieved insulin independence, although the majority of patients (82%) presented graft survival (C-peptide positivity) (30). Islet transplantation still faces major challenges, especially those related to cell loss during the process of islet isolation and the losses related to the graft site, apoptosis, allorejection, autoimmunity, and immunosuppression. In addition, glucose toxicity (40) and the abnormal transplant environment (17) are likely to contribute to the dysfunction of transplanted β-cells. Chronic hyperglycemia causes excess ER stress that induces β-cell apoptosis (9,41). Understanding the transplant environment is therefore important for understanding the molecular mechanism of glucose toxicity of β-cells.

Kennedy et al. reported that human β-cells in a transplant site show UPR changes in gene expression that protect against the proapoptotic effects of unfolded proteins (15). They evaluated the expression of genes involved in ER stress in β-cell-enriched tissue obtained with laser capture microdissection (LCM) from frozen sections of pancreases obtained from nondiabetic subjects at surgery (control) and from human islets transplanted into imprinting control region-severe combined immunodeficient (ICR-SCID) mice. The transplanted β-cells were exposed to mild hyperglycemia since mice have higher glucose levels than humans. RNA was extracted from the LCM specimens and microarray analysis was performed. The transplanted β-cells showed a UPR. Many genes of the IRE1 pathway that provide protection against the harmful effects of ER stress were observed to be activated, thus increasing the expression of ER chaperones and ER-associated protein degradation (ERAD) proteins. The IRE1 pathway is important in insulin biosynthesis in which transient increases in insulin production lead to IRE1 activation (37). However, the chronic activation of IRE1 during prolonged increases in insulin biosynthesis may lead to β-cell death through IRE1-mediated activation of JNK (19). However, two genes known to contribute to apoptosis, CHOP and JNK, were downregulated in this study. It is striking that β-cells in a transplant site exhibit UPR with changes that should help the cells adapt to unfolded proteins and to resist apoptosis.

Another factor that causes ER stress in transplanted β-cells is immunosuppressants. Johnson et al. showed that 24-h exposure to FK506 (tacrolimus) or mycophenolate mofetil (MMF), but not rapamycin, impairs glucose-stimulated insulin secretion in human islets. FK506 also could have acute and direct effects on islet function, whereas MMF does not. Increased cleaved caspase-3 protein levels are a hallmark of β-cell apoptosis. Caspase-3 cleavage is increased by FK506, MMF, and rapamycin (13). As CHOP is the transcriptional factor that plays an essential role in β-cell apoptosis (24), MMF and rapamycin induced CHOP expression. However, treating human islets with the glucagon-like peptide-1 (GLP-1) receptor agonist exenatide ameliorates the immunosuppressant-

induced defects in glucose-stimulated insulin release (13). The GLP-1 receptor agonist was reported to significantly reduce biochemical markers of islet ER stress in vivo. This suggests that GLP-1 receptor signaling directly modulates the ER stress response leading to promotion of β-cell adaptation and survival (43). In addition, GLP-1 receptor agonists protect β-cells against FFAs through the induction of the ER chaperone BiP and the antiapoptotic protein JunB, which mediate β-cell survival under lipotoxic conditions (7). Another report revealed that chronic GLP-1 analog liraglutide treatment increased the expression of antioxidant genes and reduced ER stress-related genes in β-cells of db/db mice (35).

Islet transplantation is one of the promising therapeutic approaches for type 1 diabetic patients. Future investigations must clarify the pathophysiology of transplanted β-cells. A better understanding of ER stress and its management is therefore required in order to maintain the transplanted β-cell function.

ACKNOWLEDGMENT: The authors declare no conflicts of interest.

REFERENCES

1. Akerfeldt, M. C.; Howes, J.; Chan, J. Y.; Stevens, V. A.; Boubenna, N.; McGuire, H. M.; King, C.; Biden, T. J.; Laybutt, D. R. Cytokine-induced β-cell death is independent of endoplasmic reticulum stress signaling. Diabetes 57(11):3034–3044; 2008.
2. Araki, E.; Oyadomari, S.; Mori, M. Impact of endoplasmic reticulum stress pathway on pancreatic beta-cells and diabetes mellitus. Exp. Biol. Med. 228(10):1213–1217; 2003.
3. Bertolotti, A.; Zhang, Y.; Hendershot, L.M.; Harding, H. P.; Ron, D. Dynamic interaction of BiP and ER stress transducers in the unfolded-protein response. Nat. Cell Biol. 2(6):326–332; 2000.
4. Butler, A. E.; Janson, J.; Bonner-Weir, S.; Ritzel, R.; Rizza, R. A.; Butler, P. C. β-cell deficit and increased β-cell apoptosis in humans with type 2diabetes. Diabetes 52(1):102–110; 2003.
5. Cardozo, A. K.; Ortis, F.; Storling, J.; Feng, Y. M.; Rasschaert, J.; Tonnesen, M.; Van Eylen, F.; Mandrup-Poulsen, T.; Herchuelz, A.; Eizirik, D. L. Cytokines downregulate the sarcoendoplasmic reticulum pump Ca^{2+} ATPase 2b and deplete endoplasmic reticulum Ca^{2+}, leading to induction of endoplasmic reticulum stress in pancreatic β-cells. Diabetes 54(2):452–461; 2005.
6. Cnop, M.; Welsh, N.; Jonas, J. C.; Jörns, A.; Lenzen, S.; Eizirik, D. L. Mechanisms of pancreatic beta-cell death in type 1 and type 2 diabetes: Many differences, few similarities. Diabetes 54(Suppl2):S97–S107; 2005.
7. Cunha, D.A.; Ladrière, L.; Ortis, F.; Igoillo-Esteve, M.; Gurzov, E. N.; Lupi, R.; Marchetti, P.; Eizirik, D. L.; Cnop, M. Glucagon-like peptide-1 agonists protect pancreatic β-cells from lipotoxic endoplasmic reticulum stress through upregulation of BiP and JunB. Diabetes 58(12): 2851–2862; 2009.
8. Donath, M. Y.; Halban, P. A. Decreased β-cell mass in diabetes: Significance, mechanisms and therapeutic implications. Diabetologia 47(3):581–589; 2004.
9. Eizirik, D. L.; Cardozo, A. K.; Cnop, M. The role for endoplasmic reticulum stress in diabetes mellitus. Endocr. Rev. 29:42–61; 2008.
10. Fonseca, S. G.; Burcin, M.; Gromada, J.; Urano, F. Endoplasmic reticulum stress in β-cells and development of diabetes. Curr. Opin. Pharmacol. 9(6):63–70; 2009.
11. Gregor, M. F.; Hotamisligil, G. S. Adipocyte stress: The endoplasmic reticulum and metabolic disease. J. Lipid Res. 48:1905–1914; 2007
12. Halban, P. A.; German, M. S.; Kahn, S. E.; Weir, G. C. Current status of islet cell replacement and regeneration therapy. J. Clin. Endocrinol. Metab. 95(3):1034–1043; 2010.
13. Johnson, J. D.; Ao, Z.; Ao, P.; Li, H.; Dai, L. J.; He, Z.; Tee, M.; Potter, K. J.; Klimek, A. M.; Meloche, R. M.; Thompson, D. M.; Verchere, C. B.; Warnock, G. L. Different effects of FK506, rapamycin, and mycophenolate mofetil on glucose-stimulated insulin release and apoptosis in human islets. Cell Transplant. 8(8):833–845; 2009.
14. Jörns, A.; Günther, A.; Hedrich, H. J.; Wedekind, D.; Tiedge, M.; Lenzen, S. Immune cell infiltration, cytokine expression, and β-cell apoptosis during the development of type 1 diabetes in the spontaneously diabetic LEW.1AR1/Ztm-iddm rat. Diabetes 54(7):2041–2052; 2005.
15. Kennedy, J.; Katsuta, H.; Jung, M. H.; Marselli, L.; Goldfine, A. B.; Balis, U. J.; Sgroi, D.; Bonner-Weir, S.; Weir, G. C. Protective unfolded protein response in human pancreatic β-cells transplanted into mice. PLoS One 5(6): e11211; 2010.
16. Klöppel, G.; Löhr, M.; Habich, K.; Oberholzer, M.; Heitz, P. U. Islet pathology and the pathogenesis of type 1 and type 2 diabetes mellitus revisited. Surv. Synth. Pathol. Res. 4(2):110–125; 1985.
17. Lau, J.; Henriksnäs, J.; Svensson, J.; Carlsson, P. O. Oxygenation of islets and its role in transplantation. Curr. Opin. Organ Transplant. 14(6):688–693; 2009.
18. Laybutt, D. R.; Preston, A. M.; Akerfeldt, M. C.; Kench, J. G.; Busch, A. K.; Biankin, A. V.; Biden, T. J. Endoplasmic reticulum stress contributes to β-cell apoptosis in type 2 diabetes. Diabetologia 50(4):752–763; 2007.
19. Lipson, K. L.; Fonseca, S. G.; Ishigaki, S.; Nguyen, L. X.; Foss, E.; Bortell, R.; Rossini, A. A.; Urano, F. Regulation of insulin biosynthesis in pancreatic β-cells by an endoplasmic reticulum-resident protein kinase IRE1. Cell Metab. 4(3):245–254; 2006.
20. Maedler, K.; Spinas, G. A.; Dyntar, D.; Moritz, W.; Kaiser, N.; Donath, M. Y. Distinct effects of saturated and monounsaturated fatty acids on β-cell turnover and function. Diabetes 50(1):69–76; 2001.
21. Maris, M.; Overbergh, L.; Gysemans, C.; Waget, A.; Cardozo, A. K.; Verdrengh, E.; Cunha, J. P.; Gotoh, T.; Cnop, M.; Eizirik, D. L.; Burcelin, R.; Mathieu, C. Deletion of C/EBP homologous protein (Chop) in C57Bl/6 mice dissociates obesity from insulin resistance. Diabetologia 55(4):1167–1178; 2012.
22. Nakatani, Y.; Kaneto, H.; Kawamori, D.; Yoshiuchi, K.; Hatazaki, M.; Matsuoka, T. A.; Ozawa, K.; Ogawa, S.; Hori, M.; Yamasaki, Y.; Matsuhisa, M. Involvement of endoplasmic reticulum stress in insulin resistance and diabetes. J. Biol. Chem. 280(1):847–851; 2005.
23. Oslowski, C. M.; Urano, F. The binary switch that controls the life and death decisions of ER stressed β-cells. Curr. Opin. Cell Biol. 23(2):207–215, 2011.
24. Oyadomari, S.; Koizumi, A.; Takeda, K.; Gotoh, T.; Akira, S.; Araki, E.; Mori, M. Targeted disruption of the Chop

gene delays endoplasmic reticulum stress-mediated diabetes. J. Clin. Invest. 109(4):525–532; 2002.
25. Oyadomari, S.; Takeda, K.; Takiguchi, M.; Gotoh, T.; Matsumoto, M.; Wada, I.; Akira, S.; Araki, E.; Mori, M. Nitric oxide-induced apoptosis in pancreatic β-cells is mediated by the endoplasmic reticulum stress pathway. Proc. Natl. Acad. Sci. USA 98(19):10845–10850; 2001.
26. Ozcan, U.; Cao, Q.; Yilmaz, E.; Lee, A. H.; Iwakoshi, N. N.; Ozdelen, E.; Tuncman, G.; Görgün, C.; Glimcher, L. H.; Hotamisligil, G. S. Endoplasmic reticulum stress links obesity, insulin action, and type 2 diabetes. Science 306(5695):457–461; 2004.
27. Rhodes, C. J. Type 2 diabetes—a matter of β-cell life and death? Science 307(5708):380–384; 2005.
28. Ron, D.; Walter, P. Signal integration in the endoplasmic reticulum unfolded protein response. Nat. Rev. Mol. Cell Biol. 8(7):519–529; 2007.
29. Rutkowski, D. T.; Kaufman, R. J. That which does not kill me makes me stronger: Adapting to chronic ER stress. Trends Biochem. Sci. 32(10):469–476; 2007.
30. Ryan, E. A.; Paty, B. W.; Senior, P. A.; Bigam, D.; Alfadhli, E.; Kneteman, N. M.; Lakey, J. R.; Shapiro, A. M. Five-year follow-up after clinical islet transplantation. Diabetes 54(7):2060–2069; 2005.
31. Sage, A. T.; Holtby-Ottenhof, S.; Shi, Y.; Damjanovic, S.; Sharma, A. M.; Werstuck, G. H. Metabolic syndrome and acute hyperglycemia are associated with endoplasmic reticulum stress in human mononuclear cells. Obesity 20(4):748–755; 2012.
32. Scheuner, D.; Kaufman, R. J. The unfolded protein response: A pathway that links insulin demand with β-cell failure and diabetes. Endocr. Rev. 29(3):317–333; 2008.
33. Shapiro, A. M.; Lakey, J. R.; Ryan, E. A.; Korbutt, G. S.; Toth, E.; Warnock, G. L.; Kneteman, N. M.; Rajotte, R. V. Islet transplantation in seven patients with type 1 diabetes mellitus using a glucocorticoid-free immunosuppressive regimen. N. Engl. J. Med. 343(4):230–238; 2000.
34. Shimabukuro, M.; Zhou, Y. T.; Levi, M.; Unger, R. H. Fatty acid-induced beta cell apoptosis: A link between obesity and diabetes. Proc. Natl. Acad. Sci. USA 95(5):2498–2502; 1998.
35. Shimoda, M.; Kanda, Y.; Hamamoto, S.; Tawaramoto, K.; Hashiramoto, M.; Matsuki, M.; Kaku, K. The human glucagon-like peptide-1 analogue liraglutide preserves pancreatic β-cells via regulation of cell kinetics and suppression of oxidative and endoplasmic reticulum stress in a mouse model of diabetes. Diabetologia 54(5):1098–1108; 2011.
36. Uno, S.; Imagawa, A.; Okita, K.; Sayama, K.; Moriwaki, M.; Iwahashi, H.; Yamagata, K.; Tamura, S.; Matsuzawa, Y.; Hanafusa, T.; Miyagawa, J.; Shimomura, I. Macrophages and dendritic cells infiltrating islets with or without β-cells produce tumor necrosis factor-alpha inpatients with recent-onset type 1 diabetes. Diabetologia 50(3):596–601; 2007
37. Urano, F.; Wang, X.; Bertolotti, A.; Zhang, Y.; Chung, P.; Harding, H. P.; Ron, D. Coupling of stress in the ER to activation of JNK protein kinases by transmembrane protein kinase IRE1. Science 287(5453):664–666; 2000.
38. Wang, Q.; Zhang, H.; Zhao, B.; Fei, H. IL-1beta caused pancreatic β-cells apoptosis is mediated in part by endoplasmic reticulum stress via the induction of endoplasmic reticulum Ca^{2+} release through the c-Jun N-terminal kinase pathway. Mol. Cell. Biochem. 324(1–2):183–190; 2009.
39. Wang, X. Z.; Lawson, B.; Brewer, J. W.; Zinszner, H.; Sanjay, A.; Mi, L. J.; Boorstein, R.; Kreibich, G.; Hendershot, L. M.; Ron, D. Signals from the stressed endoplasmic reticulum induce C/EBP-homologous protein (CHOP/GADD153). Mol. Cell Biol. 16(8):4273–4280; 1996.
40. Weir, G. C.; Bonner-Weir, S. Five stages of evolving β-cell dysfunction during progression to diabetes. Diabetes 53(Suppl 3):S16–S21; 2004.
41. Weir, G. C.; Marselli, L.; Marchetti, P.; Katsuta, H.; Jung, M. H.; Bonner-Weir, S. Towards better understanding of the contributions of overwork and glucotoxicity to the beta-cell inadequacy of type 2 diabetes. Diabetes Obes. Metab. 11(4):82–90; 2009.
42. Wu, J.; Kaufman, R. J. From acute ER stress to physiological roles of the unfolded protein response. Cell Death Differ. 13(3):374–384; 2006.
43. Yusta, B.; Baggio, L. L.; Estall, J. L.; Koehler, J. A.; Holland, D. P.; Li, H.; Pipeleers, D.; Ling, Z.; Drucker, D. J. GLP-1 receptor activation improves β-cell function and survival following induction of endoplasmic reticulum stress. Cell Metab. 4(5):391–406; 2006.

Cell Medicine, Vol. 5, pp. 69–73, 2013
Printed in the USA.

2155-1790/13 $90.00 + .00
DOI: http://dx.doi.org/10.3727/215517913X666503
www.cognizantcommunication.com

Isolation Efficiency of Mouse Pancreatic Stem Cells Is Age Dependent

Takashi Kuise,* Hirofumi Noguchi,† Issei Saitoh,‡ Hitomi Usui Kataoka,§
Masami Watanabe,¶ Yasufumi Noguchi,# and Toshiyoshi Fujiwara*

*Department of Gastroenterological Surgery, Okayama University Graduate School of Medicine, Dentistry and Pharmaceutical Sciences, Okayama, Japan
†Department of Surgery, Clinical Research Center, Chiba-East Hospital, National Hospital Organization, Chiba, Japan
‡Department of Pediatric Dentistry, Niigata University Graduate School of Medical and Dental Sciences, Niigata, Japan
§Department of Primary Care and Medical Education, Okayama University Graduate School of Medicine, Dentistry and Pharmaceutical Sciences, Okayama, Japan
¶Department of Urology, Okayama University Graduate School of Medicine, Dentistry and Pharmaceutical Sciences, Okayama, Japan
#Department of Socio-environmental Design, Hiroshima International University, Hiroshima, Japan

Mouse pancreatic stem cells have been isolated from mouse pancreata. This study evaluated the efficacy of isolating mouse pancreatic stem cells using mice of different ages. The pancreata of newborn mice, 8-week-old mice, and 24-week-old mice were harvested and digested by using collagenase. The "duct-like" cells in the digested pancreatic tissue were then inoculated into 96-well plates, cloned by limiting dilution, and cultured in DMEM with 20% FBS. Pancreatic stem cells were isolated from the pancreata of all newborn mice, while cells could only be isolated from 10% of the pancreata of 8-week-old mice and could not be isolated from the pancreata of any 24-week-old mice. These data suggest that young mice may have some pancreatic stem cells and that older mice may only have a few pancreatic stem cells. These data also indicate that it is extremely difficult to isolate pancreatic stem cells from older mice, suggesting that future research focus its efforts on finding methods of isolating pancreatic stem cells from adult mice.

Key words: Mouse pancreatic stem cells; Age dependent; Diabetes; ES medium; Feeder cells; Pancreatic islet transplantation

INTRODUCTION

Diabetes is one of the most increasingly prevalent and serious metabolic diseases. The reduction of insulin biosynthesis by pancreatic β-cells is closely associated with the onset and progression of diabetes. It is therefore important to search for ways to produce sufficient numbers of insulin-producing cells for transplantation in diabetes. While there is renewed interest in islet transplantation due to the recent success of this procedure (8,12,16,17,19,20,22), efforts are hindered by the limited supply of donor pancreata. Pancreatic stem/progenitor cells could become a useful tool for β-cell replacement therapy in diabetic patients since the cells are abundantly available in the pancreas of these patients and in donor organs. It was thought that pancreatic stem/progenitor cells were predominantly derived from the precursor cells residing among pancreatic epithelial duct cells or duct-associated cells both during embryonic development and later in life (1). Islet cell neogenesis from ducts has been observed in experimental injury models in rats (1,26) and in transgenic mice overexpressing certain growth factors or cytokines (5,23,27). Mouse pancreatic stem cells were recently established from the pancreata of newborn mice without genetic manipulation (17). These pancreatic stem cells have the potential to differentiate into not only insulin-producing cells but also hepatocytes (17,27). The isolation technique used might be useful for identification and isolation of human pancreatic stem/progenitor cells. This study attempted to isolate pancreatic stem cells from the pancreata of newborn mice, 8-week-old mice, and 24-week-old mice, in order to evaluate the isolation efficiency of mouse pancreatic stem cells.

Received June 1, 2012; final acceptance May 1, 2013. Online prepub date: May 14, 2013.
Address correspondence to Hirofumi Noguchi, M.D., Ph.D., Department of Surgery, Clinical Research Center, Chiba-East National Hospital, National Hospital Organization, 673 Nitona, Chuo-ku, Chiba 260-8712, Japan. Tel: +81-43-261-5171; Fax: +81-43-268-2613; E-mail: n.hirofumi@cehpnet.com *or* noguchih2006@yahoo.co.jp

MATERIALS AND METHODS

Isolation and Culture of Mouse Pancreatic Stem Cells and Islets

The review committee of Okayama University Graduate School of Medicine, Dentistry and Pharmaceutical Sciences approved these studies. Islets were removed from newborn (0-week-old), 8-week-old, and 24-week-old C57BL/6 mice (CLEA Japan, Inc., Meguro, Tokyo, Japan) using a modified method reported previously (17). Briefly, 2 ml of cold M199 medium (Life Technologies Japan, Tokyo, Japan) containing 2 mg/ml collagenase (Roche Boehringer Mannheim, Indianapolis, IN, USA) was injected into the cannulated common bile duct (14). The pancreas was removed, and an Optiprep® density gradient (Sigma-Aldrich, St. Louis, MO, USA) was used to isolate the islets.

The tissue collagenase was digested (2 mg/ml) and cultured in Dulbecco's modified Eagle's medium (DMEM; Life Technologies Japan) with 20% lot-limited fetal bovine serum (FBS; BIO-WEST, Inc., Logan, UT, USA; S1560 Lot. #SO5094S1560). Once the cells had attached and spread, cells with a fibroblast morphology (nonductal cells) were removed using a rubberscrapper (Life Technologies Japan). The "duct-like" cells were cultured in DMEM with 20% FBS in 96-well plates (Life Technologies Japan) and cloned by limiting dilution.

After single cell cloning, the mouse pancreatic stem cells were maintained in specific culture condition with lot-limited FBS (17) during the early studies (first study using a 0-week-old pancreas and first to fifth studies using 8-week-old pancreata) or in culture condition of mouse ES cells (18) during the later studies (studies except first study using a 0-week-old pancreas and first to fifth studies using 8-week-old pancreata).

The current study maintained mouse pancreatic stem cells in DMEM with 20% FBS (BIO-WEST, Inc., S1560 Lot. #SO5094S1560) during the early studies (first study using a 0-week-old pancreas and first to fifth studies using 8-week-old pancreata) or complete ES cell media with 15% FBS (Millipore, Billerica, MA, USA) on feeder layers of mitomycin C (Sigma-Aldrich)-treated STO cells [Sandos inbred mice fibroblast cell line with 6-thioguanine and ouabain resistance; American Type Culture Collection (ATCC), Manassas, VA, USA] during the later studies (studies except first study using a 0-week-old pancreas and first to fifth studies using 8-week-old pancreata).

ES Cell Culture and Differentiation

Mouse ES cells (ATCC) were maintained in and differentiated using a modification of a method that was reported previously (3,7,17). ES cells differentiated into definitive endoderm in stage 1, into gut tube endoderm in stage 2, and into pancreatic progenitors in stage 3.

Semiquantitative RT-PCR

Total RNA was extracted from cells using a method that was reported previously (13). Semiquantitative RT-PCR was performed using a modification of a method that was reported previously (17). In brief, the RNA was reverse-transcribed into cDNA using SuperScript II Reverse Transcriptase (Life Technologies Japan). Polymerization reactions were performed in a Perkin-Elmer 9700 Thermocycler with 3 µl cDNA (20 ng RNA equivalents), 160 µmol/L cold dNTPs, 10 pmol appropriate oligonucleotide primers, 1.5 mmol/L $MgCl_2$, and 5 U AmpliTaq Gold DNA polymerase (Perkin-Elmer, Norwalk, CT, USA). The oligonucleotide primers and cycle number used for semiquantitative PCR are shown in Table 1. The steps taken to vali-date these measurements were previously reported (13).

Cell Induction and Differentiation Into Insulin-Producing Cells

Cell induction was performed using a modification of a method that was reported previously (17). In brief, the cells were cultured in DMEM with 10% FBS, 10 nM exendin-4, 10 mM nicotinamide, 10 ng/ml keratinocyte growth factor (KGF; all from Sigma-Aldrich), 100 nM pancreatic and duodenal homeobox factor 1 (Pdx1) protein, and 100 nM β-cell E-box transactivator/neuronal differentiation 1 (BETA2/NeuroD) proteins for 2 weeks. Pdx1 and BETA2/NeuroD proteins were generated by cDNA as previously described (18).

Table 1. List of Gene-Specific Primers

Gene	Forward/Reverse Primer
Sox17	ctgccctgccgggatggcacggaatc/ttctggccctcaggtcg ggtcggcaac
Foxa2	tggtcactggggacaagggaa/gcaacaacagcaatagagaac
Hnf1β	cacagccctcaccagcagcc/gactgcctgggctctgctgc
Hnf4α	acacgtccccatctgaaggtg/cttccttcttcatgccagccc
Pdx1	cctgcgtgcctgtacatggg/tttccacgcgtgagctttgg
Hnf6	gggtgagccatgagccggtg/catagccgcgccgggatgag
Insulin-1	ccagctataatcagagacca/gtgtagaagaagccacgct
Insulin-2	tccgctacaatcaaaaaccat/gctgggtagtggtgggtcta
Glucagon	actcacagggcacattcacc/ccagttgatgaagtccctgg
NeuroD	gcgctcaggcaaaagccc/gccattgatgctgagcggcg
Pax6	cagtcacagcggagtgaatc/cgcttcagctgaagtcgcat
Isl-1	agatatgggagacatgggcgat/acacagcggaaacactcgatg
GAPDH	accacagtccatgccatcac/tccaccaccctgttgctgta

Sox 17, sex-determining region Y-box17; Foxa2, forkhead box protein a2; Hnf, hepatocyte nuclear factor; Pdx1; pancreatic and duodenal homeobox factor-1; NeuroD, neuronal differentiation 1; Isl-1, Islet or Insulin gene enhancer protein; Pax6, paired box gene 6; GAPDH, glyceraldehyde-3-phosphate dehydrogenase.

RESULTS

Isolation of Pancreatic Stem Cells

Pancreatic stem cells were isolated from all three pancreata from newborn mice (efficacy: 100%). On the other hand, pancreatic stem cells were isolated from only 3 of 30 pancreata of 8-week-old mice (10%) and from none of the 30 pancreata of 24-week-old mice (0%, Table 2). Each pancreatic stem cell formed "cobblestone" morphology (Fig. 1).

Growth Activity of the Pancreatic Stem Cells

One of the pancreatic stem cells from each isolate, named HN#101, HN#111, HN#121, HN#13, HN#21, or HN#23, was evaluated for growth activity. Each cell divided actively beyond population doubling level (PDL) 100 (passage 25) without growth inhibition (Fig. 2). These data suggest that pancreatic stem cells from different aged mice have a similar growth activity.

Gene Expression of the Pancreatic Stem Cells

An RT-PCR analysis of endodermal/pancreatic progenitor cell markers was performed to investigate gene expression in each clone. Differentiated cells from ES cells, generated by a stepwise differentiation protocol that relies on intermediates thought to be similar to cell populations present in the developing embryo (3,7), were used as a positive control. The marker gene expression patterns of the definitive endoderm [sex-determining region Y-box17 (Sox17), forkhead box protein a2 (Foxa2)], gut tube endoderm [hepatocyte nuclear factor 1β (HNF1β), HNF4α], and pancreatic progenitors (Hnf6, Pdx1) were detected in each cell (Fig. 3). These data suggest similar gene expression in each cell culture.

Differentiation Ability of the Pancreatic Stem Cells

HN#101, HN#111, HN#121 (all 0 week) and HN#13, HN#21, or HN#23 (all 8 weeks) cells were induced to differentiate into insulin-producing cells by Pdx1 and BETA2/NeuroD protein transduction (11,13) with exendin-4 for 2 weeks. Treatment induced the expression of insulin-2, BETA2/NeuroD, islet 1 (Isl-1), and paired box 6 (Pax6) transcription factors and glucagon in the differentiated cells (Fig. 4). These data suggest that each clone could differentiate into insulin-producing cells.

Table 2. Isolation Efficacy of Mouse Pancreatic Stem Cells

	Old	Suc#/Iso#	Clone#	Name
Mouse	0 w	3/3 (100%)	6	HN#101–106
			4	HN#111–114
			8	HN#121–128
Mouse	8 w	3/30 (10%)	15	HN#1–15
			7	HN#21–27
			3	HN#31–33
Mouse	24 w	0/30 (0%)		

Suc#/Iso#, successful isolation number of pancreatic stem cells/total isolation number; w, weeks.

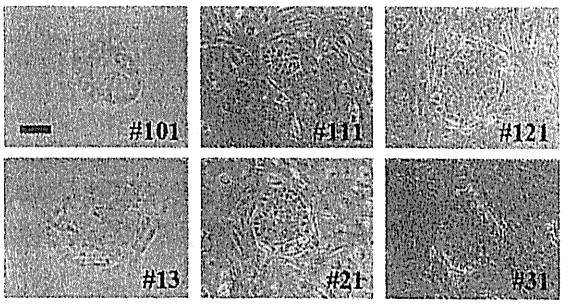

Figure 1. Isolation and culture of pancreatic stem cells. Morphology of pancreatic stem cells from newborn (HN#101, HN#111, HN#121) and 8-week-old mice (HN#13, HN#21, HN#31). The "duct-like" cells from digested pancreatic tissue were inoculated onto 96-well plates, cloned by limiting dilution, and cultured in DMEM with 20% FBS or complete ES cell media on feeder layers of mitomycin C-treated STO cells (Sandos inbred mice fibroblast cell line with 6-thioguanine and ouabain resistance). Scale bar: 100 μm.

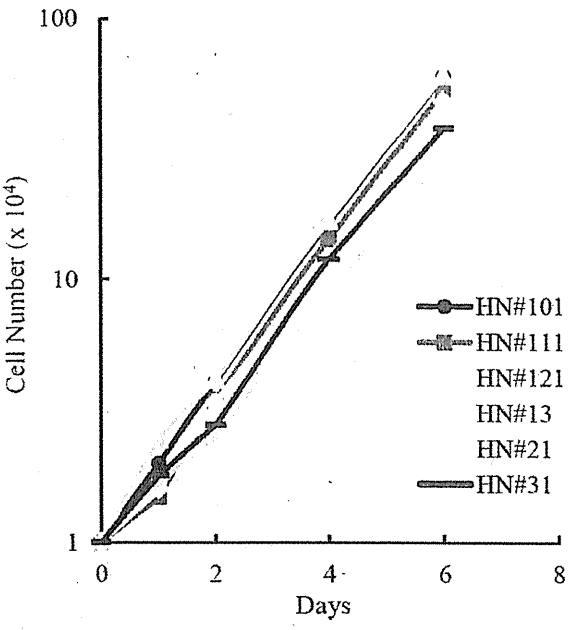

Figure 2. Growth activity of the pancreatic stem cells. HN#101, HN#111, HN#121, HN#13, HN#21, and HN#31 cells were cultured in complete ES cell media on feeder layers of mitomycin C-treated STO cells and evaluated for their growth activity.

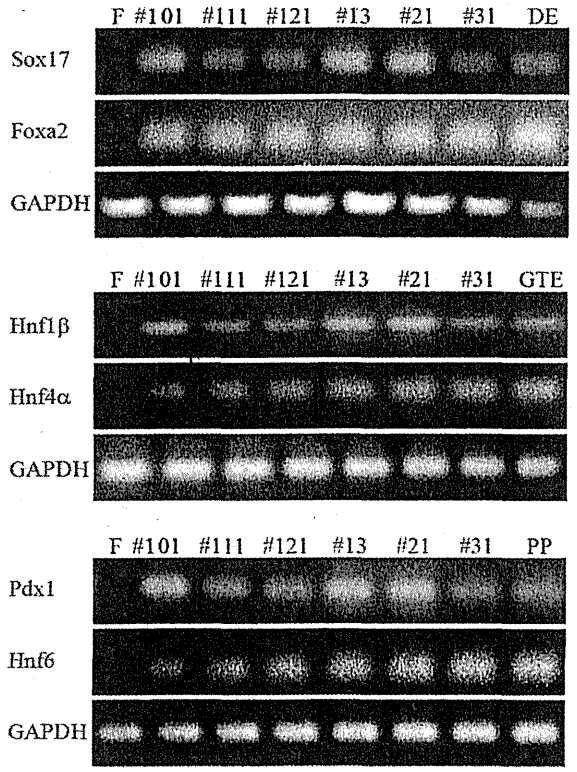

Figure 3. Gene expression of the pancreatic stem cells in culture condition 3. RT-PCR analysis of endodermal/pancreatic progenitor cell markers was used to investigate gene expression in HN#101, HN#102, HN#103, HN#13, HN#21, and HN#31 cells. F, feeder cells (STO cells, negative control); #101, HN#101 cells at PDL 100; #111, HN#111 cells at PDL 100; #121, HN#121 cells at PDL 100; #13, HN#13 cells at PDL 100; #21, HN#21 cells at PDL 100; #31, HN#31 cells at PDL 100; DE, differentiated definitive endoderm cells from ES cells (positive control); GTE, differentiated gut tube endoderm cells from ES cells (positive control); PP, differentiated pancreatic progenitors cells from ES cells (positive control); Sox17, sex-determining region Y box 17; Foxa2, forkhead box A2; GAPDH, glyceraldehyde 3-phosphate dehydrogenase; Hnf, hepatocyte growth factor; Pdx1, pancreatic and duodenal homeobox factor 1.

DISCUSSION

This study evaluated the isolation efficacy of mouse pancreatic stem cells. Pancreatic stem cells were isolated from the pancreata of all newborn mice. On the other hand, the isolation efficacy of pancreatic stem cells from 8-week-old mice was only 10% and 0% from 24-week-old mice. These data suggest that young mice may have many pancreatic stem cells, while older mice may have only a few pancreatic stem cells. It is also extremely difficult to get clones of pancreatic stem cells from older mice. Indeed, human pancreatic stem cells could not be isolated from 20- to 60-year-old donors (15). Although it is not possible to conclude that there are few human pancreatic stem cells in older donors because the culture conditions for maintenance of human pancreatic stem cells have not yet been established, the evidence from mouse pancreatic stem cells may explain why human pancreatic stem cells have not been isolated from older donors.

As the number of diabetic patients continues to increase worldwide, pancreatic stem/progenitor cells could become a useful tool for β-cell replacement therapy since the cells are abundantly available in the pancreas of these patients and in donor organs (2,4,6,9,10,11,13,15,21,24,25). However, the technique for the isolation of pancreatic stem cells remains difficult, and it is necessary to find a more efficient process. The current study suggests that it is extremely difficult to isolate pancreatic stem cells from the pancreata of older mice, in particular. Furthermore, since the optimal culture conditions for the maintenance of human pancreatic stem cells have yet to be established,

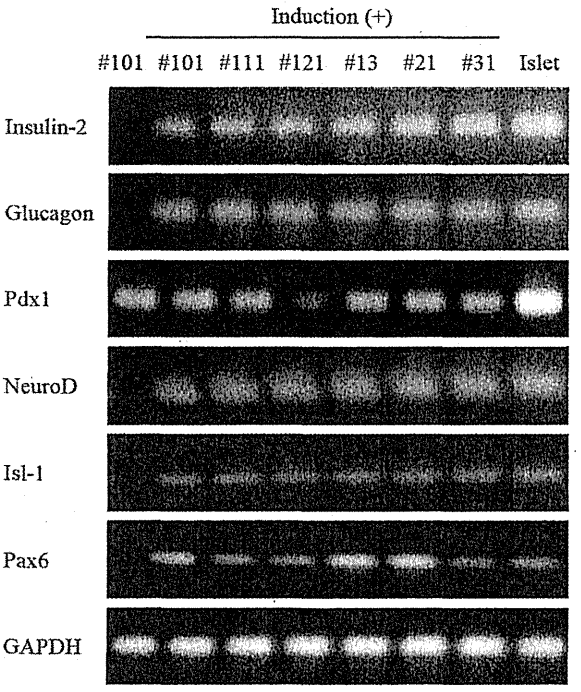

Figure 4. Differentiation ability of the pancreatic stem cells after culture for 2 months. HN#101, HN#102, HN#103, HN#13, HN#21, and HN#31 cells were induced to differentiate into insulin-producing cells using 10 nM exendin-4, 10 mM nicotinamide, 10 ng/ml KGF, 100 nM Pdx1 protein, and 100 nM BETA2/NeuroD protein for 2 weeks. PCR was performed in a Perkin-Elmer 9700 Thermocycler with 2 μl cDNA (20 ng RNA equivalent) from the cells. The oligonucleotide primers and cycle number used for semiquantitative PCR are shown in Table 1. #101, HN#101 cells at PDL 100; #111, HN#111 cells at PDL 100; #121, HN#121 cells at PDL 100; #13, HN#13 cells at PDL 100; #21, HN#21 cells at PDL 100; #31, HN#31 cells at PDL 100; Islet, mouse islets (positive control); Isl-1, islet 1; Pax6, paired homeobox 6.

the current data may suggest that it will be extremely difficult to isolate human pancreatic stem cells. Further optimization of methods is needed to isolate human pancreatic stem cells and to maintain the undifferentiated fate of human pancreatic stem cells.

ACKNOWLEDGMENTS: The authors wish to thank Mr. Koji Oda and Ms. Noriko Imagawa (Okayama University) for their valuable technical support. This work was supported in part by the Japan Society for the Promotion of Science. The authors declare no conflict of interest.

REFERENCES

1. Bonner-Weir, S.; Baxter, L. A.; Schuppin, G. T.; Smith, F. E. A second pathway for regeneration of adult exocrine and endocrine pancreas: A possible recapitulation of embryonic development. Diabetes 42:1715–1720; 1993.
2. Bonner-Weir, S.; Taneja, M.; Weir, G. C.; Tatarkiewicz, K.; Song, K. H.; Sharma, A.; O'Neil, J. J. In vitro cultivation of human islets from expanded ductal tissue. Proc. Natl. Acad. Sci. USA 97:7999–8004; 2000.
3. D'Amour, K. A.; Banq, A. G.; Eliazer, S.; Kelly, O. G.; Aqulnick, A. D.; Smart, N. G.; Moorman, M. A.; Kroon, E.; Carpenter, M. K.; Baetqe, E. E. Production of pancreatic hormone-expressing endocrine cells from human embryonic stem cells. Nat. Biotechnol. 24:1392–1401; 2006.
4. Edlund, H. Pancreas: How to get there from the gut? Curr. Opin. Cell Biol. 11:663–668; 1999.
5. Gu, D.; Sarvetnick, N. Epithelial cell proliferation and islet neogenesis in IFN-gamma transgenic mice. Development 118:33–46; 1993.
6. Heremans, Y.; Van De Casteele, M.; in't Veld, P.; Gradwohl, G.; Serup, P.; Madsen, O.; Pipeleers, D.; Heimberg, H. Recapitulation of embryonic neuroendocrine differentiation in adult human pancreatic duct cells expressing neurogenin 3. J. Cell Biol. 159:303–312; 2002.
7. Kroon, E.; Martinson, L. A.; Kadoya, K.; Banq, A. G.; Kelly, O. G.; Eliazer, S.; Young, H.; Richardson, M.; Smart, N. G.; Cunninqham, J.; Aqulnick, A. D.; D'Amour, K. A.; Carpenter, M. K.; Baetqe, E. E. Pancreatic endoderm derived from human embryonic stem cells generates glucose-responsive insulin-secreting cells in vivo. Nat. Biotechnol. 26:443–452; 2008.
8. Kuise, T.; Noguchi, H. Recent progress in pancreatic islet transplantation. World J. Transplant. 1:13–18; 2011.
9. Noguchi, H. Pancreatic stem/progenitor cells for the treatment of diabetes. Rev. Diabet. Stud. 7:105–111; 2010.
10. Noguchi, H. Production of pancreatic beta-cells from stem cells. Curr. Diabetes Rev. 6:184–190; 2010.
11. Noguchi, H.; Bonner-Weir, S.; Wei, F. Y.; Matsushita, M.; Matsumoto, S. BETA2/NeuroD protein can be transduced into cells due to an arginine- and lysine-rich sequence. Diabetes 54:2859–2866; 2005.
12. Noguchi, H.; Iwanaga, Y.; Okitsu, T.; Nagata, H.; Yonekawa, Y.; Matsumoto, S. Evaluation of islet transplantation from non-heart beating donors. Am. J. Transplant. 6:2476–2482; 2006.
13. Noguchi, H.; Kaneto, H.; Weir, G. C.; Bonner-Weir, S. PDX-1 protein containing its own antennapedia-like protein transduction domain can transduce pancreatic duct and islet cells. Diabetes 52:1732–1737; 2003.
14. Noguchi, H.; Matsushita, M.; Okitsu, T.; Moriwaki, A.; Tomizawa, K.; Kang, S.; Li, S. T.; Kobayashi, N.; Matsumoto, S.; Tanaka, K.; Tanaka, N.; Matsui, H. A new cell-permeable peptide allows successful allogeneic islet transplantation in mice. Nat. Med. 10:305–309; 2004.
15. Noguchi, H.; Naziruddin, B.; Jackson, A.; Shimoda, M.; Ikemoto, T.; Fujita, Y.; Chujo, D.; Takita, M.; Kobayashi, N.; Onaca, N.; Hayashi, S.; Levy, M. F.; Matsumoto, S. Characterization of human pancreatic progenitor cells. Cell Transplant. 19:879–886; 2010.
16. Noguchi, H.; Naziruddin, B.; Shimoda, M.; Chujo, D.; Takita, M.; Sugimoto, K.; Itoh, T.; Onaca, N.; Levy, M. F.; Matsumoto, S. A combined continuous density/osmolality gradient for supplemental purification of human islets. Cell Med. 3:33–41; 2012.
17. Noguchi H.; Oishi K.; Ueda M.; Yukawa H.; Hayashi S.; Kobayashi N.; Levy M. F.; Matusmoto S. Establishment of mouse pancreatic stem cell line. Cell Transplant. 18:563–571; 2009.
18. Noguchi, H.; Saitoh, I.; Kataoka, H. U.; Watanabe, M.; Noguchi, N.; Fujiwara, T. Culture conditions of mouse pancreatic stem cells. Cell Med. 5:63-68; 2013.
19. Noguchi, H.; Ueda, M.; Hayashi, S.; Kobayashi, N.; Nagata, H.; Iwanaga, Y.; Okitsu, T.; Matsumoto, S. Comparison of M-Kyoto solution and histidine-tryptophan-ketoglutarate solution with a trypsin inhibitor for pancreas preservation in islet transplantation. Transplantation 84:655–658; 2007.
20. Noguchi, H.; Ueda, M.; Nakai, Y.; Iwanaga, Y.; Okitsu, T.; Nagata, H.; Yonekawa, Y.; Kobayashi, N.; Nakamura, T.; Wada, H.; Matsumoto, S. Modified two-layer preservation method (M-Kyoto/PFC) improves islet yields in islet isolation. Am. J. Transplant. 6:496–504; 2006.
21. Noguchi, H.; Xu, G.; Matsumoto, S.; Kaneto, H.; Kobayashi, N.; Bonner-Weir, S.; Hayashi, S. Induction of pancreatic stem/progenitor cells into insulin-producing cells by adenoviral-mediated gene transfer technology. Cell Transplant. 15:929–938; 2006.
22. Shapiro, A. M.; Lakey, J. R.; Ryan, E. A.; Korbutt, G. S.; Toth, E.; Warnock, G. L.; Kneteman, N. M.; Rajotte, R. V. Islet transplantation in seven patients with type 1 diabetes mellitus using a glucocorticoid-free immunosuppressive regimen. N. Engl. J. Med. 343:230–238; 2000.
23. Song, S. Y.; Gannon, M.; Washington, M. K.; Scoqqins, C. R.; Meszoely, I. M.; Goldenring, J. R.; Marino, C. R.; Sandqren, E. P.; Coffey, Jr., R. J.; Wright, C. V.; Leach, S. D. Expansion of Pdx1-expressing pancreatic epithelium and islet neogenesis in transgenic mice overexpressing transforming growth factor α. Gastroenterology 117:1416–1426; 1999.
24. Street, C. N.; Lakey, J. R.; Shapiro, A. M.; Imes, S.; Rajotte, R. V.; Ryan, E. A.; Lyon, J. G.; Kin, T.; Avila, J.; Tsujimura, T.; Korbutt, G. S. Islet graft assessment in the Edmonton Protocol: Implications for predicting long-term clinical outcome. Diabetes 53:3107–3114; 2004.
25. Suzuki, A.; Nakauchi, H.; Taniguchi, H. Prospective isolation of multipotent pancreatic progenitors using flow-cytometric cell sorting. Diabetes 53:2143–2152; 2004.
26. Wang, R. N.; Kloppel, G.; Bouwens, L. Duct- to islet-cell differentiation and islet growth in the pancreas of duct-ligated adult rats. Diabetologia 38:1405–1411; 1995.
27. Yamamoto, T.; Yamato, E.; Taniguchi, H.; Shimoda, M.; Tashiro, F.; Hosoi, M.; Sato, T.; Fujii, S.; Miyazaki, J. I. Stimulation of cAMP signaling allows isolation of clonal pancreatic precursor cells from adult mouse pancreas. Diabetologia 49:2359–2367; 2006.

Cell Medicine, Vol. 5, pp. 63–68, 2013
Printed in the USA.

2155-1790/13 $90.00 + .00
DOI: http://dx.doi.org/10.3727/215517913X666495
www.cognizantcommunication.com

Culture Conditions for Mouse Pancreatic Stem Cells

Hirofumi Noguchi,* Issei Saitoh,† Hitomi Usui Kataoka,‡ Masami Watanabe,§
Yasufumi Noguchi,¶ and Toshiyoshi Fujiwara#

*Department of Surgery, Clinical Research Center, Chiba-East Hospital, National Hospital Organization, Chiba, Japan
†Department of Pediatric Dentistry, Niigata University Graduate School of Medical and Dental Sciences, Niigata, Japan
‡Department of Primary Care and Medical Education, Okayama University Graduate School of Medicine, Dentistry and Pharmaceutical Sciences, Okayama, Japan
§Department of Urology, Okayama University Graduate School of Medicine, Dentistry and Pharmaceutical Sciences, Okayama, Japan
¶Department of Socio-environmental Design, Hiroshima International University, Hiroshima, Japan
#Department of Gastroenterological Surgery, Okayama University Graduate School of Medicine, Dentistry and Pharmaceutical Sciences, Okayama, Japan

Recently, mouse pancreatic stem cells have been isolated from adult mouse pancreata. However, these pancreatic stem cells could be maintained only under specific culture conditions with lot-limited fetal bovine serum (FBS). For the efficient isolation and maintenance of mouse pancreatic stem cells, it is important to identify culture conditions that can be used independent of the FBS lot. In this study, we evaluated the culture conditions required to maintain mouse pancreatic stem cells. The mouse pancreatic stem cells derived from the pancreas of a newborn mouse, HN#101, were cultured under the following conditions: 1) Dulbecco's modified Eagle's medium (DMEM) with 20% lot-limited FBS, in which mouse pancreatic stem cells could be cultured without changes in morphology and growth activity; 2) complete embryonic stem (ES) cell media; and 3) complete ES cell media on feeder layers of mitomycin C-treated STO cells, which were the same culture conditions used for mouse ES cells. Under culture conditions #1 and #3, the HN#101 cells continued to form a flat "cobblestone" monolayer and continued to divide actively beyond the population doubling level (PDL) 100 without growth inhibition, but this did not occur under culture condition #2. The gene expression profile and differentiated capacity of the HN#101 cells cultured for 2 months under culture condition #3 were similar to those of HN#101 cells at PDL 50. These data suggest that complete ES cell media on feeder layers could be useful for maintaining the undifferentiated state of pancreatic stem cells.

Key words: Mouse pancreatic stem cells; Culture condition; Embryonic stem cells; Embryonic stem (ES) medium; Feeder cells; Pancreatic islet transplantation

INTRODUCTION

β-Cell replacement therapy via islet transplantation represents a promising treatment for type 1 diabetes (6,11,16–18,21). However, such an approach is severely limited by the shortage of donor organs. Pancreatic stem/progenitor cells could be a useful target for β-cell replacement therapy in diabetic patients, since the cells are abundantly available in the pancreas of these patients as well as in donor organs. We recently established mouse pancreatic stem cells without genetic manipulation (19). The clonal cell line obtained (HN#13) expresses the pancreatic and duodenal homeobox factor 1 (Pdx1), also known as islet/duodenal homeobox-1 (IDX-1)/somatostatin transcription factor 1 (STF-1)/insulin promoter factor 1 (IPF1), one of the transcription factors specific for the β-cell lineage. Induction therapy with exendin-4 and with the Pdx1 and β-cell E-box transactivator/neuronal differentiation 1 (BETA2/NeuroD) transcription factors using protein transduction technology (9,10,12–14) stimulated the expression of insulin mRNA in the cells. Yamamoto et al. also reported the generation of mouse pancreatic stem cells using serum-free medium containing cholera toxin, which stimulated cAMP signaling in the cells (24). These pancreatic stem cells have the potential to differentiate into not only insulin-producing cells but also hepatocytes (19,24). These isolation techniques might also be useful for the identification and isolation of human pancreatic stem/progenitor cells.

On the other hand, the HN#13 cells could be maintained in Dulbecco's modified Eagle's medium (DMEM) with only 1 of 10 different lots of fetal bovine serum (FBS) (BIO-

Received June 1, 2012; final acceptance May 1, 2013. Online prepub date: May 14, 2013.
Address correspondence to Hirofumi Noguchi, M.D., Ph.D., Department of Surgery, Clinical Research Center, Chiba-East National Hospital, National Hospital Organization, 673 Nitona, Chuo-ku, Chiba 260-8712, Japan. Tel: +81-43-261-5171; Fax: +81-43-268-2613;
E-mail: n.hirofumi@cehpnet.com *or* noguchih2006@yahoo.co.jp

WEST, Inc., Logan, UT, USA; S1560 Lot. #SO5094S1560). The cells in the other DMEM-FBS formed "fibroblast-like" or "spindle" structures and stopped dividing after three to six passages (19). For efficient isolation and maintenance of mouse pancreatic stem cells, it is important to identify culture conditions that are independent of the FBS lot. In this study, we evaluated the culture conditions required to maintain mouse pancreatic stem cells.

MATERIALS AND METHODS

Isolation and Culture of Mouse Pancreatic Stem Cells and Islets

The mouse studies were approved by the review committee of Okayama University Graduate School of Medicine, Dentistry and Pharmaceutical Sciences. Islets were isolated from the pancreata of 8-week-old mice (C57BL/6; CLEA Japan, Inc., Meguro, Tokyo, Japan). For islet isolation,the common bile duct was cannulated and injected with 2 ml of cold M199 medium (Life Technologies Japan, Tokyo, Japan) containing 2 mg/ml collagenase (Roche Boehringer Mannheim, Indianapolis, IN, USA) (14). The islets were separated on a density gradient (Optiprep®, Sigma-Aldrich, St. Louis, MO, USA), hand-picked under a dissecting microscope to ensure a pure islet preparation, and used immediately afterward.

Pancreatic stem cells from newborn mice were isolated using a modification of a method that was reported previously (19). In brief, the pancreatic tissue from newborn mice was digested by 2 mg/ml collagenase, and the digested cells were then cultured in DMEM (Life Technologies) with 20% FBS (BIO-WEST, Inc., S1560 Lot. #SO5094S1560). After the cells were attached and spread, nonductal cells (fibroblast morphology) were removed mechanically with a rubberscrapper (Life Technologies). The "duct-like" cells were then inoculated into 96-well plates (Life Technologies), cloned by limiting dilution, and cultured in DMEM with 20% FBS.

Culture Conditions

Mouse pancreatic stem cells from newborn mice were cultured under the following conditions: 1) DMEM with 20% FBS(BIO-WEST, Inc., S1560 Lot. #SO5094S1560), 2) complete embryonic stem (ES) cell media with 15% FBS (Millipore, Billerica, MA, USA), 3) complete ES cell media with 15% FBS on feeder layers of mitomycin C (Sigma-Aldrich)-treated STO cells [Sandos inbred mice fibroblast cell line with 6-thioguanine and ouabain resistance; American Type Culture Collection (ATCC), Manassas, VA, USA] (the same as the culture conditions used for mouse ES cells) (Fig. 1A).

ES Cell Culture and Differentiation

Mouse ES cells (ATCC) were maintained in complete ES cell media with 15% FBS on feeder layers of mitomycin C-treated STO cells. ES cells were passaged every 3 days. The cells that differentiated from ES cells (generated by a stepwise differentiation protocol that relies on intermediates thought to be similar to cell populations present in the developing embryo) were used as a positive control. Directed differentiation was conducted as described previously (2,5), with minor modifications. In stage 1, cells were treated with 25 ng/ml of wingless-type MMTV integration site family, member 3A (Wnt3a) and 100 ng/ml of activin A (R&D Systems, Minneapolis, MN, USA) in Roswell Park Memorial Institute media (RPMI; Life Technologies) for 1 day, followed by treatment with 100 ng/ml of activin A in RPMI+0.2% FBS for 2 days. In stage 2, the cells were treated with 50 ng/ml of fibroblast growth factor 10 (FGF10; R&D Systems) and 0.25 μM of 3-keto-*N*-(aminoethyl-aminocaproyl-dihydrocinnamoyl) cyclopamine (KAAD-cyclopamine; Toronto Research Chemicals, Ontario, Canada) in RPMI+2% FBS for 3 days. In stage 3, the cells were treated with 50 ng/ml of FGF10, 0.25 μM of KAAD-cyclopamine, and 2 μM of all-*trans* retinoic acid (Sigma-Aldrich, Tokyo, Japan) in DMEM+1% (v/v) B27 supplement (Life Technologies) for 3 days. ES cells differentiated into definitive endoderm in stage 1, into gut tube endoderm in stage 2, and then into pancreatic progenitors in stage 3.

Semiquantitative RT-PCR

Total RNA was extracted from cells using an RNeasy Mini Kit (QIAGEN, Tokyo, Japan). After quantifying the RNA by spectrophotometry, 2.5 μg of RNA were heated at 85°C for 3 min and then reverse-transcribed into cDNA in a 25-μl solution containing 200 U of Superscript II RNase H-RT (Life Technologies), 50 ng random hexamers (Life Technologies), 160 μmol/L dNTP, and 10 nmol/L dithiothreitol. The reaction consisted of 10 min at 25°C, 60 min at 42°C, and 10 min at 95°C. Polymerization reactions were performed in a Perkin-Elmer 9700 Thermocycler with 3 μl cDNA (20 ng RNA equivalents), 160 μmol/L cold dNTPs, 10 pmol appropriate oligonucleotide primers, 1.5 mmol/L $MgCl_2$, and 5 U of AmpliTaq Gold DNA polymerase (Perkin-Elmer, Norwalk, CT, USA). The oligonucleotide primers and cycle numbers used for semiquantitative PCR are shown in Table 1. The thermal cycle profile used a 10-min denaturing step at 94°C, followed by amplification cycles (1 min denaturation at 94°C, 1 min annealing at 57°C, and 1 min extension at 72°C) with a final extension step of 10 min at 72°C. The steps taken to validate these measurements have all been reported previously (12).

Cell Induction and Differentiation Into Insulin-Producing Cells

To induce cellular differentiation, the cells were cultured in DMEM with 10% FBS, 10 nM exendin-4, 10 mM nicotinamide, 10 ng/ml heratinocyte growth factor

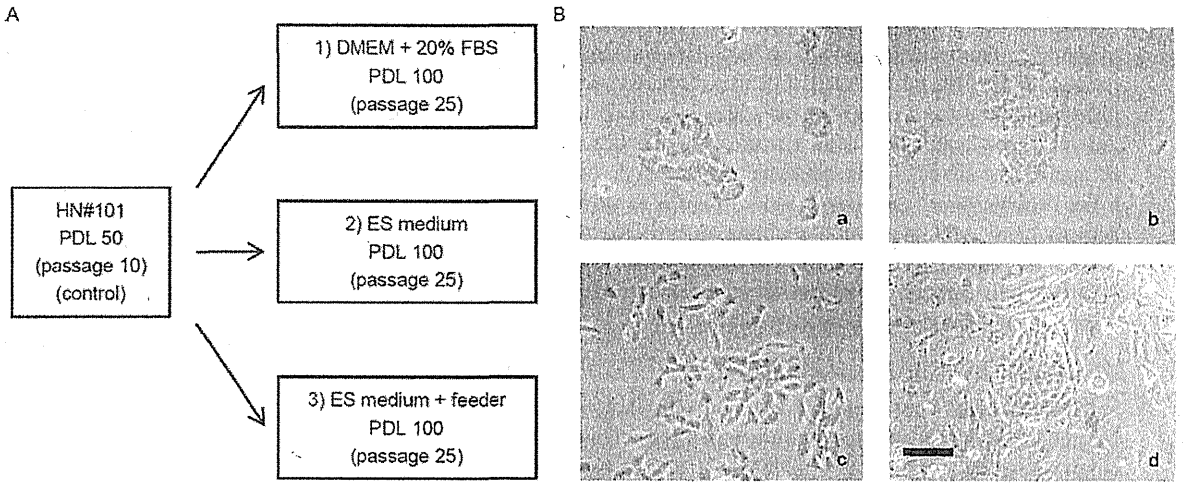

Figure 1. Isolation and culture of pancreatic stem cells. (A) Study design. HN#101 cells (PDL 50) were cultured under the following conditions: 1) DMEM with 20% FBS, 2) complete ES cell media with 15% FBS, 3) complete ES cell media with 15% FBS on feeder layers of mitomycin C-treated STO cells (the same as the culture conditions used for mouse ES cells). (B) The morphology of the pancreatic stem cells isolated from a newborn mouse, HN#101 (PDL 50). After digestion of pancreatic tissue, the "duct-like" cells were inoculated into 96-well plates, cloned by limiting dilution, and cultured in DMEM with 20% FBS. (a) The morphology of the HN#101 cells in DMEM with 20% FBS (PDL 50). (b) The morphology of the HN#101 cells in DMEM with 20% FBS (PDL 100). (c) The morphology of the HN#101 cells in complete ES cell media with 15% FBS (PDL 100). (d) The morphology of the HN#101 cells in complete ES cell media with 15% FBS on feeder layers of mitomycin C-treated STO cells (Sandos inbred mice fibroblast cell line with 6-thioguanine and ouabain resistance; PDL 100). Scale bar: 100 μm.

(KGF; all Sigma-Aldrich), 100 nM Pdx1 protein, and 100 nM BETA2/NeuroD protein for 7 to 10 days. For the Pdx1 and BETA2/NeuroD proteins, the cDNAs were amplified by PCR using appropriate linker primers and then were subcloned into the *Nde* I and *Xho* I sites of pET21b(+) (Novagen, Madison, WI, USA) using a ligation kit (TaKaRa, Tokyo, Japan). BL21 (DE3) cells (Life Technologies) containing the expression plasmids were grown at 37°C to an OD_{600} of 0.8. Next, isopropyl-β-D-thiogalactopyranoside (Sigma-Aldrich) was added to a final concentration of 0.1 mmol/L, and the cells were then incubated for 12 h at 24°C. Cells were sonicated, and the supernatants were recovered and applied to a column of Ni-nitrilotriacetic acid agarose (Life Technologies).

Table 1. List of Gene-Specific Primers

Gene	Forward/Reverse Primer
Sox17	ctgccctgccgggatggcacggaatc/ ttctggccctcaggtcgggtcggcaac
Foxa2	tggtcactggggacaagggaa/gcaacaacagcaatagagaac
Hnf1β	cacagccctcaccagcagcc/gactgcctgggctctgctgc
Hnf4α	acacgtccccatctgaaggtg/cttccttcttcatgccagccc
Pdx1	cctgcgtgcctgtacatggg/tttccacgcgtgagctttgg
Hnf6	gggtgagccatgagccggtg/catagccgcgccgggatgag
Insulin-1	ccagctataatcagagacca/gtgtagaagaagccacgct
Insulin-2	tccgctacaatcaaaaaccat/gctgggtagtggtgggtcta
Glucagon	actcacagggcacattcacc/ccagttgatgaagtccctgg
NeuroD	gcgctcaggcaaaagccc/gccattgatgctgagcggcg
Isl-1	agatatgggagacatgggcgat/acacagcggaaacactcgatg
Pax6	cagtcacagcggagtgaatc/cgcttcagctgaagtcgcat
GAPDH	accacagtccatgccatcac/tccaccaccctgttgctgta

Sox 17, sex-determining region Y-box17; Foxa2, forkhead box protein a2; Hnf, hepatocyte nuclear factor; Pdx1, pancreatic and duodenal homeobox factor-1; NeuroD, neuronal differentiation 1; Isl-1, islet or insulin gene enhancer protein; Pax6, paired box gene 6; GAPDH, glyceraldehyde-3-phosphate dehydrogenase.

RESULTS

Isolation of Pancreatic Stem Cells

Pancreatic stem cells were isolated from the pancreata of newborn mice. After digestion of pancreatic tissue, the "duct-like" cells were then inoculated into 96-well plates, cloned by limiting dilution, and cultured in DMEM with 20% FBS (see Materials and Methods for a more detailed description). Of the more than 200 isolated clones, six clones were able to be cultured for more than 3 months. One of the clones, named HN#101 (Fig. 1B-a), which formed a flat, monolayer "cobblestone" morphology, was used to evaluate the culture conditions.

Morphology of the Pancreatic Stem Cells Cultured in Different Media

We previously reported that one of the previously isolated pancreatic stem cell clones, the HN#13 cells, could be maintained during culture in DMEM using only 1 of 10 different lots of FBS (19). For efficient isolation and

maintenance of mouse pancreatic stem cells, it is important to identify culture conditions that can be used that are independent of the FBS lot. HN#101 cells were cultured under different culture conditions for their ability to support the growth of pancreatic stem cells. Under culture conditions #1 and #3, the HN#101 cells could be maintained to form a flat "cobblestone" monolayer and continued to divide actively beyond the population doubling level (PDL) 100 (over 3 months) (Fig. 1B-b, B-d). On the other hand, the HN#101 cells formed "fibroblast-like/spindle" structures when grown under culture condition #2 (Fig. 1B-c).

Growth Activity of the Pancreatic Stem Cells

HN#101 cells were evaluated for their growth activity under the three different culture conditions. Under culture conditions #1 and #3, the HN#101 cells divided actively beyond PDL 100 without growth inhibition (Fig. 2). Under culture condition #2, the growth activity of the HN#101 cells gradually decreased (Fig. 2). These data suggest that conditions #1 and #3 are suitable for the culture of mouse pancreatic stem cells.

Gene Expression Profile of the Pancreatic Stem Cells Under Culture Condition #3

To investigate the gene expression in HN#101 cells cultured for 2 months under culture condition #3, an RT-PCR analysis of endodermal/pancreatic progenitor cell markers was performed. Cells that differentiated from ES cells (generated by a stepwise differentiation protocol that relies on intermediates thought to be similar to cell populations present in the developing embryo) (2,5) were used as a positive control. The marker gene expression patterns of the definitive endoderm [sex-determining region Y-box17 (Sox17), forkhead box protein a2 (Foxa2)], gut tube endoderm [hepatocyte nuclear factor 1β (Hnf1β), Hnf4α], and pancreatic progenitors (Hnf6, Pdx1) were detected in HN#101 cells cultured for 2 months under culture condition #3 (Fig. 3). These data suggest that the gene expression pattern in HN#101 cells cultured for 2 months under culture condition #3 was similar to that of undifferentiated HN#101 cells.

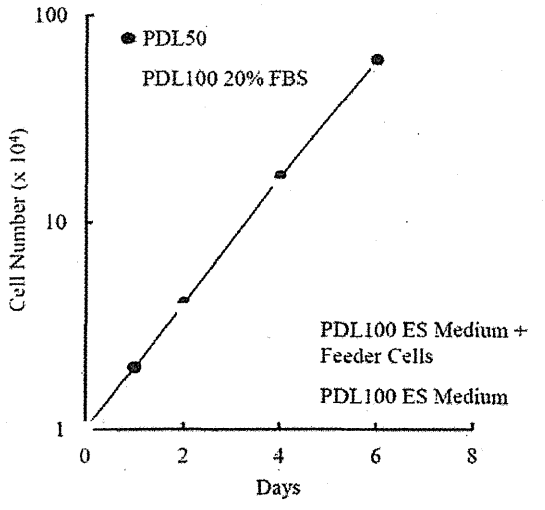

Figure 2. Growth activity of the pancreatic stem cells. HN#101 cells (PDL 50 = control) were evaluated for their growth activity under three different culture conditions (1–3 in Fig. 1). Under culture conditions #1 and #3, the HN#101 cells divided actively beyond PDL 100 without any change in growth activity. Under culture condition #2, the growth activity of the HN#101 cells was gradually decreased.

Differentiation Capacity of the Pancreatic Stem Cells After Culture for 2 Months Under Culture Condition #3

To evaluate whether the differentiation capacity of the pancreatic stem cells was maintained under culture condition #3, the HN#101 cells cultured for 2 months under culture condition #3 were induced to differentiate into insulin-producing cells by treatment with exendin-4, Pdx1 protein, and BETA2/NeuroD protein for 7 to 10 days. We previously reported that Pdx1 and BETA2/NeuroD protein transduction technology could be a safe and valuable strategy for facilitating the differentiation of stem/progenitor cells into insulin-producing cells without requiring the use of gene transfer technology (10,12). The treated cells induced the expression of insulin-2 mRNA (but not insulin-1 mRNA), although the level of insulin-2 mRNA was still low compared with that of primary mouse islets (Fig. 4). We also examined the expression of other transcription factors and pancreas-related genes. After induction, the expression of the BETA2/NeuroD islet-1 (Isl-1) and paired box 6 (Pax6) transcription factors and glucagon were induced (Fig. 4). These data suggest that complete ES cell media and growth of cells on feeder layers, the same culture conditions that are used for mouse ES cells, could be useful in maintaining the undifferentiated state of pancreatic stem cells.

DISCUSSION

In this study, we evaluated the culture conditions required to maintain mouse pancreatic stem cells. The complete ES cell media with 15% FBS and feeder layers of mitomycin C-treated STO cells, the same conditions that are used to culture mouse ES cells, are suitable for culturing mouse pancreatic stem cells. Since the culture in complete ES cell media without feeder cells failed to maintain the undifferentiated state of the mouse pancreatic stem cells, feeder cells appear to be essential for the maintenance of the pancreatic stem cells. On the other hand, we previously reported that the pancreatic stem cells cultured in DMEM with 9 of 10 FBS formed "fibroblast-like" or "spindle" structure and stopped dividing after three to six passages